

**ANATOMICAL MAPPING OF SEMG SIGNAL QUALITY AND
CONTROLLABILITY IN SKELETAL MUSCLE GROUPS FOR
MYOELECTRIC PROSTHESIS**

A Thesis
Presented to
The Academic Faculty

by

Jihwan Jung

In Partial Fulfillment
of the Requirements for the Degree
Master of Science in the
George W. Woodruff School of Mechanical Engineering

Georgia Institute of Technology
August 2019

COPYRIGHT © 2019 BY JIHWAN JUNG

**ANATOMICAL MAPPING OF SEMG SIGNAL QUALITY AND
CONTROLLABILITY IN SKELETAL MUSCLE GROUPS FOR
MYOELECTRIC PROSTHESIS**

Approved by:

Dr. Frank Hammond III, Advisor
School of Mechanical/Biomedical Engineering
Georgia Institute of Technology

Dr. Minoru Shinohara
School of Biological Sciences
Georgia Institute of Technology

Dr. Lewis A. Wheaton
School of Biological Sciences
Georgia Institute of Technology

Date Approved: [May 03, 2019]

To Maverick

ACKNOWLEDGEMENTS

I would first like to thank my thesis advisor Dr. Frank Hammond III of the School of Mechanical/Biomedical Engineering at Georgia Institute of Technology. The door to Prof. Hammond's office was always open whenever I ran into a trouble spot or had a question about my research or writing. He consistently allowed this paper to be my own work, but steered me in the right the direction whenever he thought I needed it.

I would also like to thank the experts who were involved in the data analysis for this research project: Dr. Minoru Shinohara and Dr. Lewis A. Wheaton who contributed to analyzing the experiment results. Without their passionate participation and input, the validation survey could not have been successfully conducted. I am gratefully indebted to their very valuable comments on this thesis.

Finally, I must express my very profound gratitude to my parents and to my colleagues, Julie Lee and Steve Choi, for providing me with unfailing support and continuous encouragement throughout my years of study and through the process of researching and writing this thesis. This accomplishment would not have been possible without them. Thank you.

TABLE OF CONTENTS

ACKNOWLEDGEMENTS	iv
LIST OF FIGURES	vi
LIST OF SYMBOLS AND ABBREVIATIONS	viii
SUMMARY	ix
Chapter 1. Introduction	1
1.1 Myoelectric Control Potential	1
1.2 Myoelectric Control Drawbacks	2
chapter 2. Preliminary Research	4
2.1 Introduction	4
2.2 EMG Signal Processing	5
2.3 ECG Artifacts in Abdominal muscle sEMG	5
2.4 EMG Onset Detection	8
2.5 EMG Instrumentation for Real-time sEMG Signal Processing	9
2.6 Discussion	11
chapter 3. Experiment	12
3.1 Subject	12
3.2 Data Collection	12
3.3 Maximum Voluntary Contraction of the Targeted Muscle Groups in Upper Body	13
3.4 Offset error of Muscle Contraction from sEMG Output Targets	14
3.5 Variance of Muscle Contraction at sEMG Output Target	15
3.6 Contraction Bandwidth of Muscle Contraction	16
Chapter 4. Experiment Result	18
4.1 Offset Error Evaluation for Individual Muscle Contraction Accuracy	18
4.2 Variance Evaluation for Individual Muscle Contraction Stability	22
4.3 Contraction Bandwidth Evaluation for Individual Muscle Contraction	27
4.4 Evaluation of Simultaneous Muscle Contraction using LT and DT	30
4.5 Post-training effect on the performance of simultaneous contraction	39
CHAPTER 5. Discussion and Conclusion	42
5.1 Discussion	42
5.2 Conclusion	44

LIST OF FIGURES

Figure 1 - On/Off control signal processing with sEMG signals from external obliques ..	7
Figure 2 - ECG artifacts removal from sEMG signals by applying high-pass filters.....	7
Figure 3 - Integrated Profile (IP) method and Teager-Kaiser energy operator (TKEO) implementation for real-time sEMG onset detection on MATLAB	9
Figure 4 - Implementation of real-time median filtering on MATLAB; The ECG artifacts were effectively removed in the baseline as highlighted in blue circle	10
Figure 5 - sEMG output target determination based on MVC level; MVC level was determined during the MVC task and the targets were computed as 3%, 6%, 13%, 25%, and 50% MVC	14
Figure 6 - Offset error in DT at each target; the target level and the actual mean level of muscle contraction are represented in black and red dashed line, respectively. a) 6% MVC target, b) 13% MVC target, c) 25% MVC target, d) 50% MVC target	15
Figure 7 - Determination of the muscle contraction bandwidth; The shaded sections represent the rise and the fall time respectively	17
Figure 8 - Effect of Visual Feedback (VF) on offset error; The subject sEMG data were averaged across the targeted muscle groups and the target levels	19
Figure 9 - Mean activation of muscle contraction for the target levels, the subject sEMG data were averaged across the muscle groups. Target levels were represented as dashed lines	19
Figure 10 - Overall effect of %MVC (Target Intensity) on offset error; the subject sEMG data were averaged across the muscle groups and the presence or the absence of VF.....	20
Figure 11 - Effect of %MVC (Target Intensity) on offset error depending on VF; left) with VF, right) without VF	20
Figure 12 - Overall effect of Muscle group on offset error; the subject sEMG data were averaged across the target levels and the presence or the absence of VF.....	21
Figure 13 - Effect of Muscle group on offset error depending on VF; left) with VF, right) without VF	21
Figure 14 - Effect of Visual Feedback (VF) on variance; The subject sEMG data were averaged across the targeted muscle groups and the target levels	23
Figure 15 - Overall effect of %MVC (Target Intensity) on variance; the subject sEMG data were averaged across the muscle groups and the presence or the absence of VF.....	23
Figure 16 - Effect of % MVC (Target Intensity) on variance depending on VF; left) with VF, right) without VF	24
Figure 17 - Overall effect of %MVC (Target Intensity) on coefficient of variation; the subject sEMG data were averaged across the muscle groups and the presence or the absence of VF	24
Figure 18 - Effect of %MVC (Target Intensity) on coefficient of variation depending on VF; left) with VF, right) without VF	25
Figure 19 - Overall effect of Muscle group on variance; the subject sEMG data were averaged across the target levels and the presence or the absence of VF.....	25
Figure 20 - Effect of Muscle group on variance depending on VF; left) with VF, right) without VF	26
Figure 21 - Overall effect of Muscle group on coefficient of variation; the subject sEMG data were averaged across the target levels and the presence or the absence of VF	26

Figure 22 - Effect of Muscle group on coefficient of variation depending on VF; left) with VF, right) without VF	27
Figure 23 - Effect of Visual Feedback (VF) on rise time and fall time; The subject sEMG data were averaged across the targeted muscle groups and the target levels. Left) rise time, Right) fall time.....	28
Figure 24 - Overall effect of % MVC (Target Intensity) on rise time and fall time; the subject sEMG data were averaged across the muscle groups and the presence or the absence of VF. Left) Rise time, Right) Fall time.....	29
Figure 25 - Effect of % MVC (Target Intensity) on rise time and fall time depending on VF; Top left) Rise time with VF, Top right) Rise time without VF, Bottom left) Fall time with VF, Bottom right) Fall time without VF.....	29
Figure 26 - Overall Effect of Muscle group on rise time and fall time; the subject sEMG data were averaged across the target levels and the presence or the absence of VF. Left) Rise time, Right) Fall time.....	30
Figure 27 - Effect of Muscle group on rise time and fall time depending on VF; Top left) Rise time with VF, Top right) Rise time without VF, Bottom left) Fall time with VF, Bottom right) Fall time without VF	30
Figure 28 - Actual mean muscle activation for achieving each target combination; 6% MVC and 25% MVC were represented in blue and red dashed line respectively.....	32
Figure 29 - The overall offset errors during simultaneous muscle contraction with LT and DT; The result was compared with the offset errors of individual muscle contractions ..	32
Figure 30 - The offset error comparison between the simultaneous and the individual muscle contraction for each target combination during simultaneous muscle contraction with LT and DT; Top left) LT 6% + DT 6%, Top right) LT 6% + DT 25%, Bottom left) LT 25% + DT	33
Figure 31 - The overall variances during simultaneous muscle contraction with LT and DT; The result was compared with the variances of individual muscle contractions	34
Figure 32 - The variances comparison between the simultaneous and the individual muscle contraction for each target combination during simultaneous muscle contraction with LT and DT; Top left) LT 6% + DT 6%, Top right) LT 6% + DT 25%, Bottom left) LT 25% + DT 6%,	35
Figure 33 - Overall rise and fall time during simultaneous muscle contraction with LT and DT; The result was compared with the rise and fall time required for individual muscle contractions. Top) Rise time, Bottom) Fall time	36
Figure 34 - The rise time comparison between the simultaneous and the individual muscle contraction for each target combination during simultaneous muscle contraction with LT and DT; Top left) LT 6% + DT 6%, Top right) LT 6% + DT 25%, Bottom left) LT 25% + DT 6%,	37
Figure 35 - The fall time comparison between the simultaneous and the individual muscle contraction for each target combination during simultaneous muscle contraction with LT and DT; Top left) LT 6% + DT 6%, Top right) LT 6% + DT 25%, Bottom left) LT 25% + DT 6%,.....	38
Figure 36 - Comparison on offset errors in LT and DT before and after training	39
Figure 37 - Comparison on variances in LT and DT before and after training	40
Figure 38 - Comparison on rise and fall time in LT and DT before and after training	41

LIST OF SYMBOLS AND ABBREVIATIONS

MES	Myoelectric Signals
sEMG	Surface Electromyography
DOF	Degrees of Freedom
PR	Pattern Recognition
MVC	Maximum Voluntary Contraction
ECG	Electrocardiogram
DT	Deltoids
PM	Pectoralis Majors
LT	Latissimus Dorsi
EO	External Obliques

SUMMARY

Myoelectric signals have been widely investigated with the increasing demand for advanced prosthetic devices over the past decades. The myoelectric signals are composed of muscle activities induced by the superpositioned motor unit action potentials and often characterized by signal to noise ratio, amplitude, rate of change, and intensity of muscle activation. They contain information of the human motion intention, which can be directly mapped into the prosthetic device control. Compared to conventional body-powered prosthetic devices driven by mechanical maneuver of body movements through cables or harnesses, myoelectric prosthetic devices are relatively easily operated due to the aid of electric power generated by MES.

This thesis presents the hardware implementation for myoelectric signal processing and the experimental evaluation of myoelectric signals to characterize the controllability of the muscle groups in the upper body for controlling the myoelectric prosthetic device. Digital filters were implemented to improve the quality of raw myoelectric signals acquired from the targeted muscle groups. The 5th order median filter implementation provided the reliable noise reduction for the electrophysiological noise observed in the abdominal muscle groups. The real-time onset detection algorithm was implemented to determine the onset and the offset of myoelectric signals and to generate discrete control signals for the prosthetic device.

The experiment was designed to investigate the adequacy of utilizing myoelectric signals from the muscle groups in the upper body—deltoids, pectoralis majors, latissimus

dorsi, and external obliques—as used in the control of myoelectric prosthetic devices. The voluntary muscle contraction capability of each targeted muscle group was evaluated during the experiment. It was demonstrated that the precise and accurate myoelectric control was achieved using the deltoids muscle group. However, the pectoralis majors and the external obliques were proven to be more appropriate to apply to fast switching on/off control. The combinations of the myoelectric signals acquired from the deltoids and the latissimus dorsi were investigated to generate multiple output stages, and 4 discrete states of myoelectric output were obtained using those muscle groups simultaneously

CHAPTER 1. INTRODUCTION

Surface Electromyography (sEMG) signals have been adopted as non-invasive control method for myoelectric prosthetic devices. Conventional myoelectric control systems have successfully characterized myoelectric activity observed with surface electrodes, but these systems are mostly limited to control one or two degrees of freedom (DOF) at a time [1, 2, 3, 4, 5]. For multifunction myoelectric control, numerous studies have been conducted to improve the accuracy and the reliability of the control scheme by using the pattern recognition (PR), logistic regression, and mathematical models describing intrinsic and extrinsic features of muscle activity [6, 7, 8, 9 10]. Despite the suggested multifunction control schemes, the control performance is not desirable yet due to the large number of electrodes, the amount of computational resources for robust the EMG feature classification, and the lack of direct EMG mapping into kinematic information. Therefore, it is the author's belief that the development of direct anatomical mapping of sEMG signals improves the current myoelectric control scheme by establishing more intuitive and cost-effective myoelectric control system.

1.1 Myoelectric Control Potential

Myoelectric signal processing techniques with the mathematical modeling approach have been suggested to sophisticatedly describe muscle activities. Many studies have successfully implemented mathematical models to analyze the physiological changes during the muscle contraction. [11, 12]. Since MES exist in the form of combined motor unit action potentials containing the information of the muscle contraction intensity and frequency, it is required to decompose and extract the information to achieve more

consistent and reliable myoelectric control system. Recently, PR techniques have been introduced to myoelectric signal processing as artificial intelligence based on machine learning is developed for improving the performance of myoelectric control. Several studies have demonstrated that the pattern recognition myoelectric control is capable of extracting sEMG features from the residual muscles of amputated limbs with the average classification accuracy over 90% for more than 5 different classes [13, 14, 15]. This advanced control system allows the wearers to perform dexterous control with multi-functional myoelectric prosthesis.

1.2 Myoelectric Control Drawbacks

Myoelectric signals are subject to change with motion artifacts, electrode displacement, skin impedance changes, and electromagnetic interference [16]. In general, setting up high high-pass cutoff frequency can reject most high-frequency contents induced by motion artifacts, but excessive high-pass filtering might cause the substantial loss of muscle contraction intensity information within high frequency content [17]. Although the current pattern recognition myoelectric control has realized multiple DOFs in myoelectric prosthesis, appropriate signal conditioning steps for classification algorithm are still required. Furthermore, the suggested control method is limited to sequential operation since most conventional classification algorithms are designed to examine the input signal sequentially to identify its current active state.

Many studies have attempted to improve the classification accuracy by increasing number of electrodes for robust EMG feature extraction. However, currently verified classification accuracy rates are mostly not achievable in the real context since they are based on offline validation from restricted laboratory environment and experiment

conditions with high computational power [18]. Also, the myoelectric control based on the PR algorithm commonly takes EMG control input from muscle groups adjacent to the attached device to obtain suitable EMG patterns for classification, which might limit the user's motion while engaging with the device.

In this study, we suggest an alternative approach of evaluating sEMG signals from different muscle groups in upper body to investigate the accessibility of each muscle contraction and the synergistic effect of the muscle combination with different muscle group pairs for developing more intuitive myoelectric control interface.

CHAPTER 2. PRELIMINARY RESEARCH

2.1 Introduction

One of the major issues of using myoelectric prosthetic devices was reported that it was challenging to recognize the current state of the device without the aid of sensory feedback [19, 20]. Preliminary research was conducted to investigate the usage of mechanotactile feedback for the upper-limb prosthetic device to improve the human subject's performance of object discrimination based on the material stiffness, the thickness, and the surface roughness. This study demonstrated that the human subjects showed the enhanced discrimination performance when the mechanotactile-based virtual proprioception was provided [21]. Since this study focused on the experimental evaluation of manipulation with the control input driven by the potentiometer, a follow-up study was conducted to utilize myoelectric signals from biceps and triceps to control soft pneumatic actuators implemented on the adaptive grasp prosthetic device. The inflation of the air chamber in the actuator was triggered by the myoelectric signals acquired from the biceps and triceps when they exceeded the predetermined threshold levels [22]. This study demonstrated that the myoelectric signals were successfully applied to the pneumatically actuated prosthetic device for 1 DOF control scheme, and implied further implementation of multiple DOF in myoelectric-controlled prosthetic devices using different muscle groups.

2.2 EMG Signal Processing

Recommended by several studies to precisely capture fundamental sEMG features, sEMG signals are collected at a 1 kHz sampling rate. One study confirms that the conventional 1kHz sampling rate is enough to avoid the aliasing effect due to undersampling [23, 24]. The myoelectric activity measured from skeletal muscle groups can be quantified by sEMG potentials ranging from 50 μ V to 20-30 mV [25]. To quantitatively analyze the collected sEMG signals, several processing steps are required including; 1) signal conditioning, 2) rectification, and 3) smoothing. During the signal conditioning stage, the collected raw sEMG signals are amplified and bandpass filtered 10-400 Hz to remove DC offset and high frequency contents induced by power sources and motion artifacts, respectively. Full-wave rectification is recommended to conserve the portion of the sEMG signal powers below the baseline. Smoothing the pre-conditioned sEMG signals requires lowpass filter implementation with a cut-off frequency less than 10 Hz to obtain a linear envelop of the sEMG profile [26].

2.3 ECG Artifacts in Abdominal muscle sEMG

Conventional myoelectric prosthetic devices typically obtain sEMG signals from muscle groups directly involved in device control, which only allows limited range of motion while controlling the device. For example, upper-limb prosthetic devices utilize different upper extremity muscles depending on levels of amputation. Although intuitive control can be developed by using adjacent muscle groups, most existing control strategies are still limited to control the device with restricted range of motion due to hardware constraints such as the lack of intuitive and reliable sEMG interface and the potential interference with the user's motion [27, 28]. To investigate the feasibility of using

anatomically mismatched muscle groups, a preliminary study has been conducted with abdominal muscle groups such as rectus abdominis and external obliques to control a split-hook device as shown in Figure 1. When the sufficient activation level in a targeted muscle group detected by single thresholding, which is the most commonly used for timing muscle activity, a servo motor implemented at each finger joint is actuated to change the joint angle. The threshold level is determined by one's MVC (Maximum Voluntary Contraction), and different levels of MVC are examined for accurate onset detection. However, as previous studies have pointed out that abdominal sEMG signals are easily corrupted by motion and ECG (Electrocardiogram) artifacts [29], additional signal conditioning steps are required for effective sEMG signal acquisition. One simple method of removing ECG artifacts from sEMG signals is applying highpass filters with the cutoff frequency at 100 Hz or higher (Figure 2). Although this simple highpass filter implementation can effectively minimize the ECG artifacts, it might cause inevitable loss of fundamental EMG components in high frequency range leading to poor EMG intensity estimation [31].

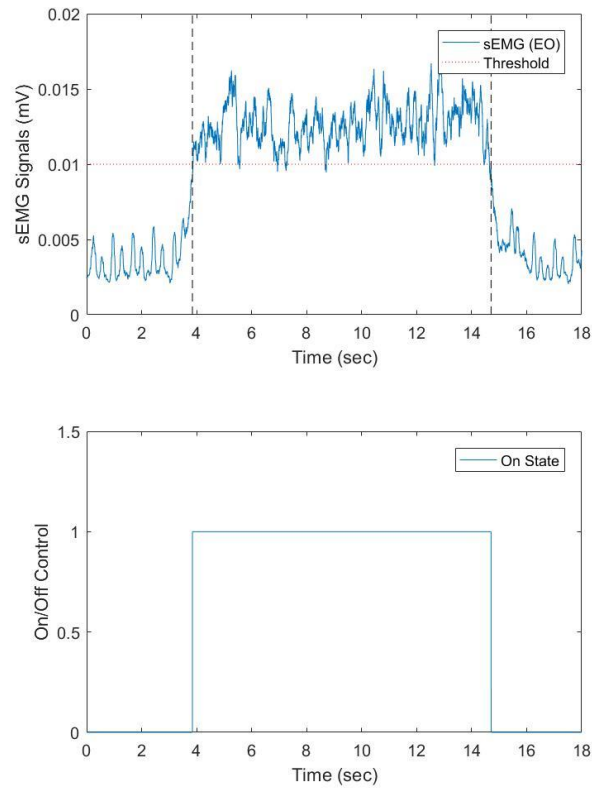


Figure 1 - On/Off control signal processing with sEMG signals from external obliques

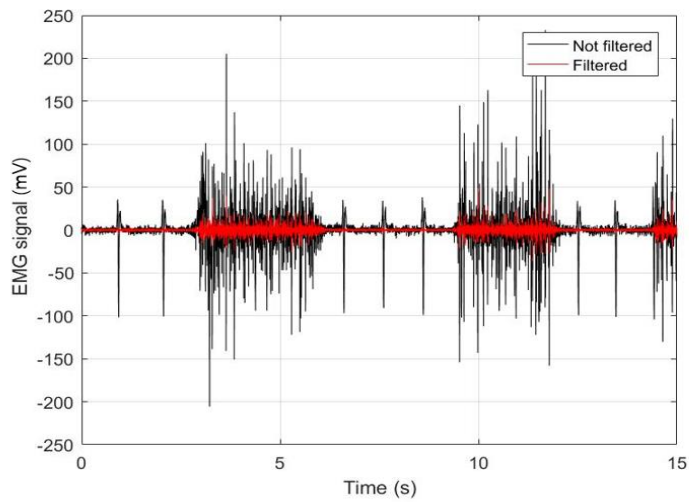


Figure 2 - ECG artifacts removal from sEMG signals by applying high-pass filters

2.4 EMG Onset Detection

The performance of onset detection with thresholding algorithm is also affected by the dominant ECG effect on abdominal sEMG signals since it is unclear to determine the threshold level under the influence of ECG artifacts. To improve the onset detection performance for sEMG signals contaminated by the artifacts, a study team developed an energy-based onset detection technique called Integrated profile (IP) method [30]. The major advantage of using IP method is that it allows reliable onset detection even for sEMG signals with large involuntary background spikes. **Figure 3** shows the demonstration of IP method implemented on MATLAB. However, it requires the continuous integrated profile of all the collected sEMG samples, which is only available with post processing. Teager–Kaiser energy operator (TKEO) is another energy-based onset detection technique suggested in a recent study which enhances the onset detection performance by improving signal to noise of the contaminated EMG signals. Whereas the TKEO method – more suitable to generate control input for manipulating myoelectric prosthetic devices in real-time--only takes the set of 3 consecutive sEMG samples for the discrete TKEO, the IP method requires the entire profile of sEMG signals for IP function computation [31].

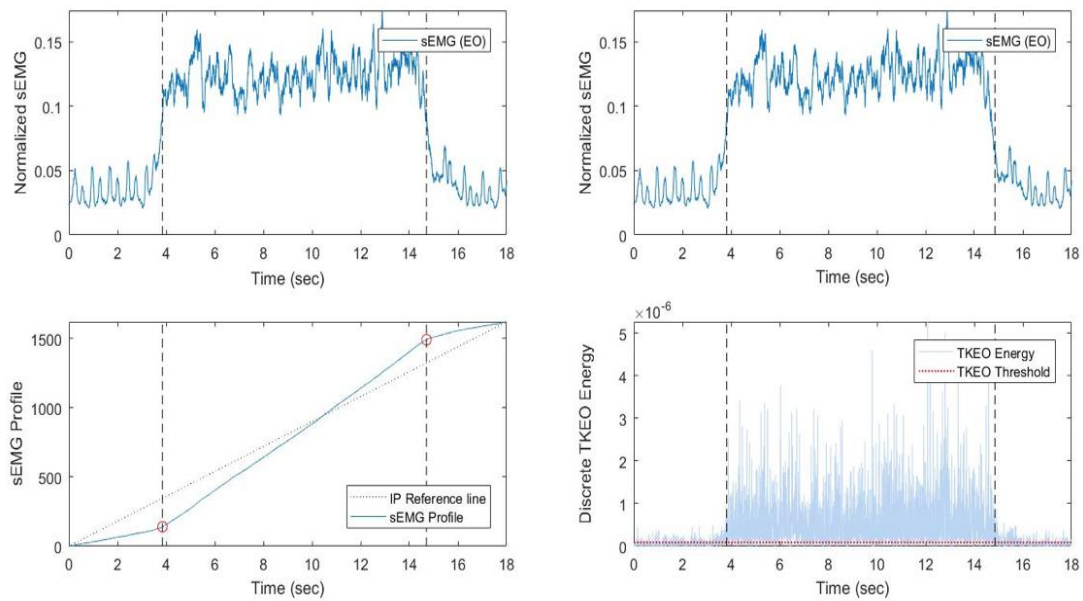


Figure 3 - Integrated Profile (IP) method and Teager-Kaiser energy operator (TKEO) implementation for real-time sEMG onset detection on MATLAB

2.5 EMG Instrumentation for Real-time sEMG Signal Processing

Myomo R&D EMG sensors were used to collect sEMG data from the targeted muscle group. The sensor consisted of two independent sensor heads and an amplifier unit with an internal preamplifier implemented. The adjustable gain of preamplifier ranges from 447x to 114100x and the default gain of 447 was applied to amplify raw sEMG signals. One sensor head was placed on the targeted muscle group and the other was used to acquire reference signals from the adjacent muscle group. The collected raw sEMG data were captured on a MSP432 LaunchPad™ microcontroller with the sampling frequency of 1 kHz and the raw sEMG data were bandpass filtered via a cascaded bandpass filter with the passband of 30-500 Hz. The sEMG data were transferred to MATLAB via UART serial communication with a baud rate of 115200. A 5TH order real-time median filter was implemented on MATLAB to remove the ECG artifacts in the baseline of the raw data, and the filtered signal was displayed on a signal monitor with an update rate of 500 Hz to

provide real-time visual feedback. Figure 4 shows implementation of real-time median filtering and demonstrates the effective removal of ECG artifacts during the muscle contractions with external obliques. The TKEO onset detection algorithm was also implemented on MATLAB to determine the onset and the offset of muscle contraction in real-time.

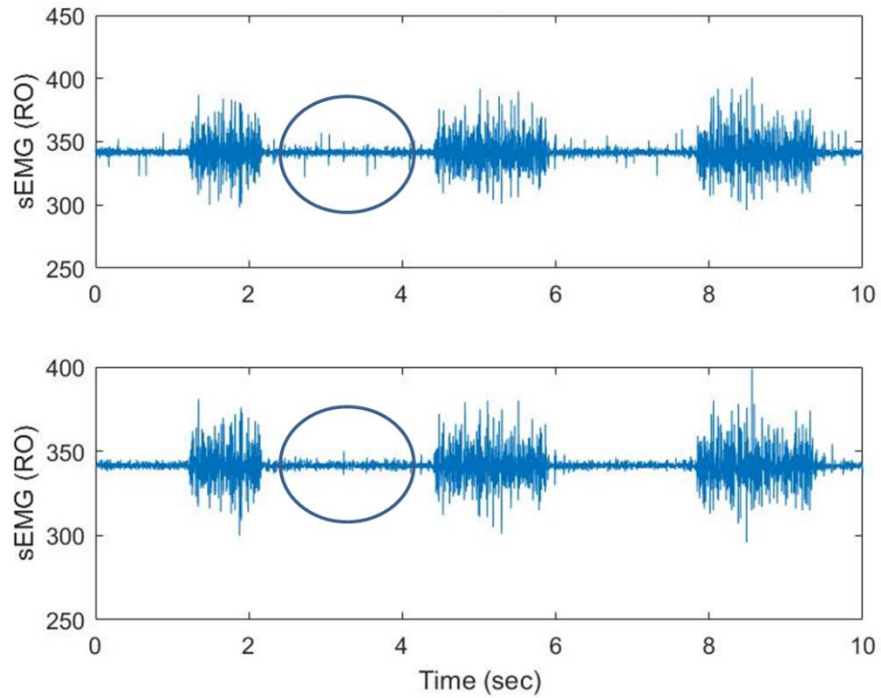


Figure 4 - Implementation of real-time median filtering on MATLAB; The ECG artifacts were effectively removed in the baseline as highlighted in blue circle

2.6 Discussion

The experimental evaluation of processing sEMG signals in real-time demonstrated that the baseline ECG artifacts were effectively removed by implementing the digital filters to acquire the desired sEMG control input for myoelectric prosthetic devices. Also, the robust sEMG onset detection was accomplished with IP method and TKEO algorithm for the corrupted sEMG signals obtained from the abdominal muscle groups. Throughout the preliminary research, it was proven that the abdominal muscle groups also can be used as the control input for the myoelectric prosthetic devices if the appropriate signal processing steps were applied to the raw sEMG signals. To extend the possibility of the sEMG signal implementation using multiple muscle groups, the sEMG signals acquired from different muscle groups in the upper-body were evaluated to achieve multiple DOF prosthetic control in the following section.

CHAPTER 3. EXPERIMENT

3.1 Subject

A total of 7 subjects participated in this study including 4 males and 3 females. All subjects had no compromised muscle capabilities such as weakened muscle contraction or limited range of motion.

3.2 Data Collection

sEMG data were collected from deltoids (DT), pectoralis majors (PM), latissimus dorsi (LT), and external obliques (EO) that represent four major muscle groups in the upper body. The subject's skin was cleaned with medical swipes to minimize the effect of bioelectrical impedance in sEMG measurement, and a pair of wet-type surface electrodes were attached to each target muscle location identified by anatomical references [32, 33]. This study focused on examining the muscles on the right side of upper body due to the inevitable interference of heart known as ECG artifacts. Then, each pair of electrodes were connected to Y03 EMG preamplifier (Y03 EMG preamplifier, Motion Lab Systems Preamplifier Incorporate), and the collected sEMG data from each targeted muscle were amplified by a factor of 300. The data acquisition interface, CED Power1401-3A (Power1401-3A, Cambridge Electronic Design), processed the incoming data from the preamplifier by using filtering tool box supported by CED Spike2 software to generate the linear envelope of sEMG signals. The lowpass cutoff frequency for smoothing raw EMG signals was set to be 5 Hz, and the processed sEMG signals were observed with the real-time signal monitor on Spike2. The MVC level of each muscle group is determined while the subject maximally contracted the targeted muscle for 10 seconds. Then, the sEMG

output targets were computed by 6%, 13%, 25%, and 50% MVC and displayed on the signal monitor to provide visual feedback for target levels of muscle contraction.

The experiment was conducted with three sessions: 1) Individual muscle contraction for the target levels using the listed muscle groups with and without visual feedback 2) Simultaneous muscle contraction for the combinations of 6% and 25% target levels using LT and DT with visual feedback, and 3) Simultaneous muscle contraction for the worst-case combination using the same muscle groups from session 2 after training. Auditory cues are provided to indicate the initiation and the termination of 10 seconds muscle contraction for each target level. During the individual muscle contraction session, the subject was first asked to achieve each target level and maintain the contraction for 10 seconds with sitting upright posture when the visual feedback is provided. Then, the subject followed the same procedure to reproduce the same target level without visual feedback, and the performance from each case was compared. The combinations used in the sessions were as follows: 1) LT 6% + DT 6% 2) LT 25% + DT 6% 3) LT 6% + DT 25% 4) LT 25% + DT 25%. During the simultaneous muscle contraction session, the subject was asked to achieve and to maintain the target levels of each combination for 10 seconds simultaneously, and the worst-case combination was determined based on the subject's response to NASA Task Load Index survey.

3.3 Maximum Voluntary Contraction of the Targeted Muscle Groups in Upper Body

The maximum voluntary contraction level of each muscle group was determined by the peak value of the recorded sEMG signals during the MVC task which requires the subject to maximally contract the targeted muscle for 10 seconds. To minimize motion artifacts during muscle contraction, each subject was asked to maintain upright sitting

posture throughout the experiment. Figure 5 shows the sEMG output targets of each muscle group computed from the MVC level. However, it is observed that the influence of ECG artifacts was predominant in the baseline of muscle contraction when the target level was set below 6% MVC. Therefore, 3% MVC target was excluded for statistical analysis on the collected sEMG data.

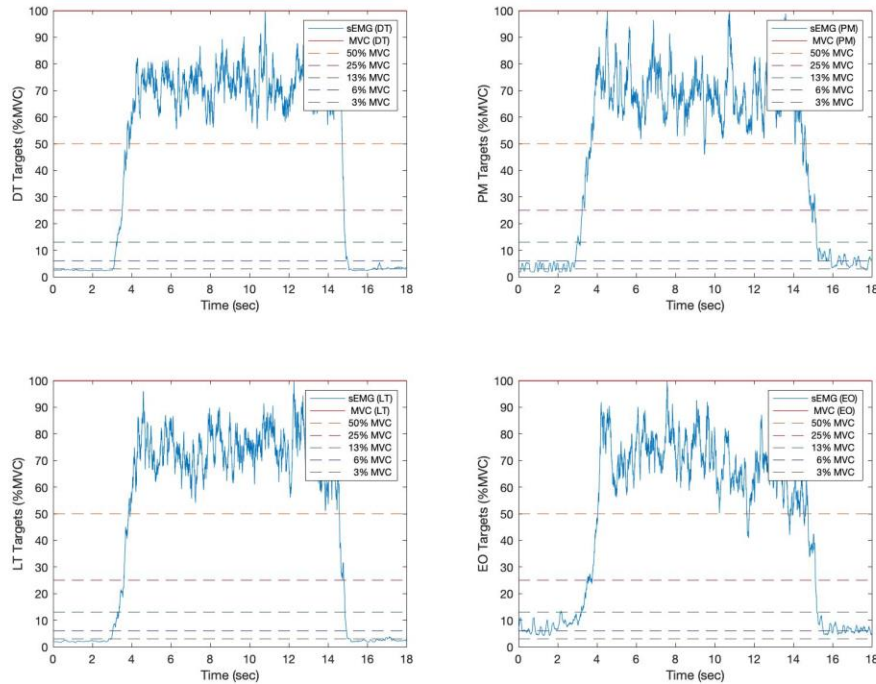


Figure 5 - sEMG output target determination based on MVC level; MVC level was determined during the MVC task and the targets were computed as 3%, 6%, 13%, 25%, and 50% MVC

3.4 Offset error of Muscle Contraction from sEMG Output Targets

To evaluate the accuracy of muscle contraction, the offset error from each target level was computed for each muscle group. Since raw sEMG data were recorded in mV, they were normalized to the MVC levels by Equation 1.

$$\text{Normalized sEMG Data} = \frac{\text{sEMG Data (mV)}}{\text{MVC (mV)}} \quad (1)$$

The IP onset detection algorithm was used to detect the onset and the offset of muscle activation and the sEMG data within the range of the onset and the offset were averaged to determine the actual mean level of the muscle activation (Equation 2). Then, the percent error between the target and the mean activation was computed to represent the offset error in %MVC (Figure 6).

$$\text{Mean Activation of Normalized sEMG} = \frac{\sum \text{Normalized sEMG Data}}{\text{Number of sEMG Data}} \quad (2)$$

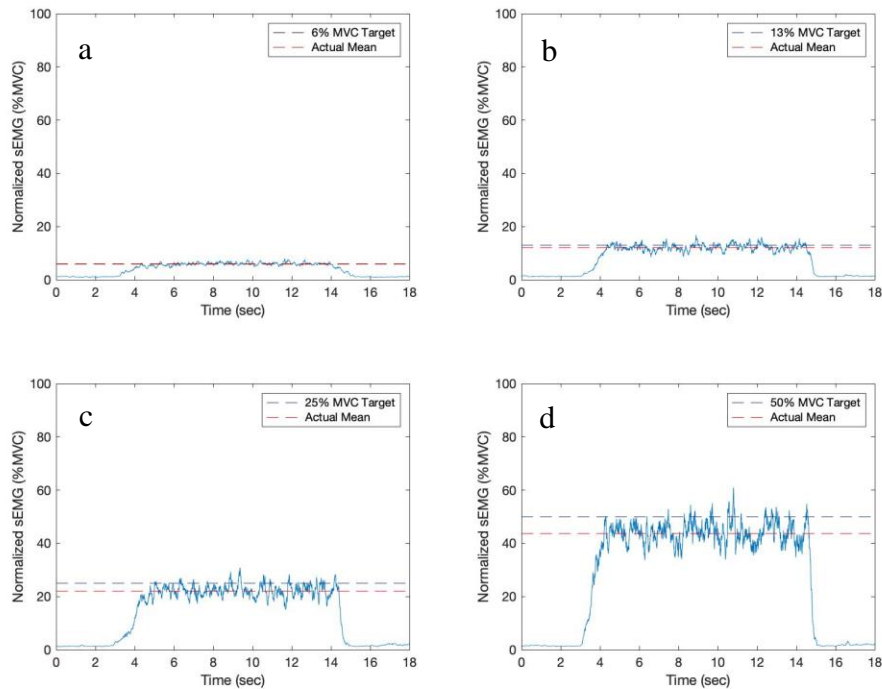


Figure 6 - Offset error in DT at each target; the target level and the actual mean level of muscle contraction are represented in black and red dashed line, respectively. a) 6% MVC target, b) 13% MVC target, c) 25% MVC target, d) 50% MVC target

3.5 Variance of Muscle Contraction at sEMG Output Target

The variance of muscle activation was analyzed to evaluate the stability of muscle contraction. The onset and offset detected by the IP detection algorithm were used to

determine the active state of muscle contraction, and the raw sEMG data were also normalized to the MVC to compute the variance during muscle activation at each target level. To compare the relative variability in sEMG signals across the subjects, the coefficient of variation was also determined by the following Equation.

$$\text{Coefficient of Variation (\%MVC}^2) = \frac{\text{Variance during the muscle activation (\%MVC}^2)}{\text{Mean activation of Normalized sEMG}} \quad (3)$$

3.6 Contraction Bandwidth of Muscle Contraction

The rise and fall time were considered to evaluate the contraction bandwidth of each muscle group. To determine the onset and offset time, three standard deviations from the baseline were used instead of the IP detection algorithm which is more appropriate to define the active state of muscle contraction at the target level. Figure 7 shows the rise and fall time were computed as the time difference between the onset and 90% of target muscle activation and between 90% of target muscle activation and the offset, respectively.

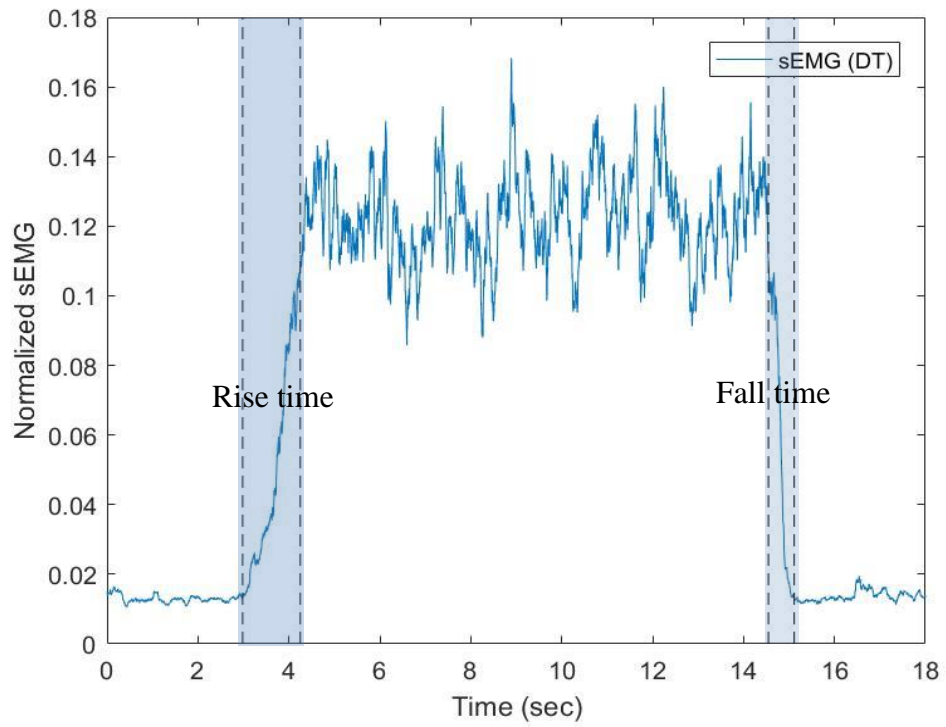


Figure 7 - Determination of the muscle contraction bandwidth; The shaded sections represent the rise and the fall time respectively

CHAPTER 4. EXPERIMENT RESULT

4.1 Offset Error Evaluation for Individual Muscle Contraction Accuracy

The offset errors were expected to increase when the visual feedback was not allowed regardless of the different muscle groups and the target levels. Figure 8 showed the effect of visual feedback on the offset error for the sEMG data averaged across the subjects, the muscle groups, and the target levels. The overall offset error was increased without the visual feedback as expected. The offset errors were conditioned on the physical properties of the muscle groups and the different levels of targets. And The increase of offset errors was likely to be found either in more intense target levels or in the muscle groups with less muscular strength. As shown in Figure 9-11, the offset errors increased exponentially as the target levels increased. The result shows the subjects were able to reduce the offset errors with the visual feedback, and they reached the targets within 10% offset deviation in all targeted muscle groups. Considering some muscle groups were more developed due to their frequent involvement in tasks of daily living, the offset errors in the muscle groups of the upper body such as DT and PM were relatively low as shown in Figure 12-13. Despite the presence of the visual feedback, the subjects still had relatively high offset errors in LT compared to the other muscle groups. Although the offset errors in EO were similar to DT and PM with the visual feedback, they were drastically increased when visual feedback was not permitted.

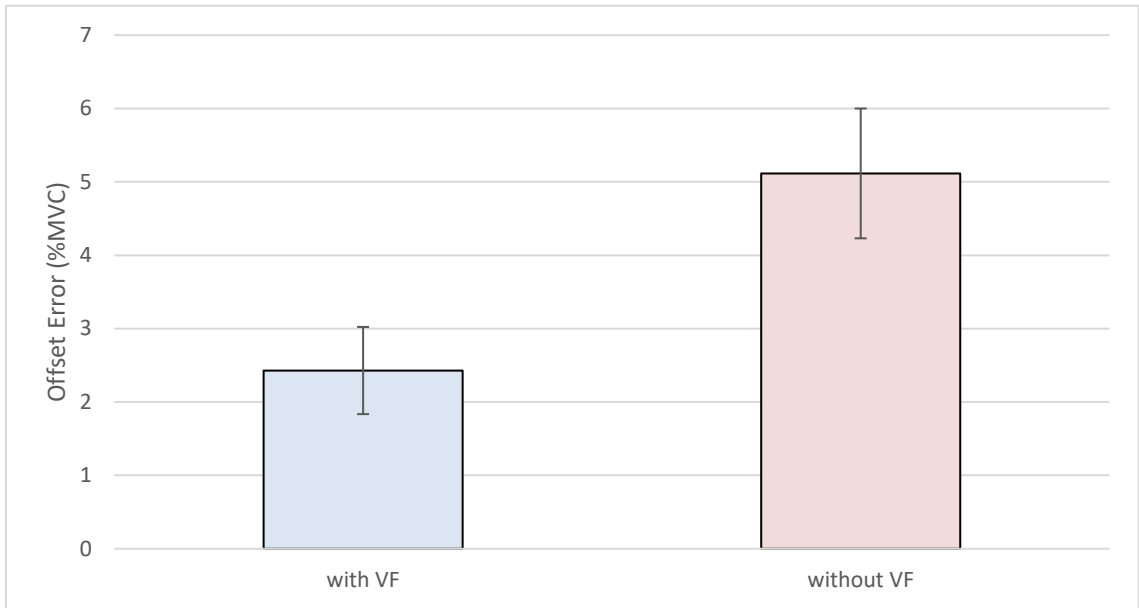


Figure 8 - Effect of Visual Feedback (VF) on offset error; The subject sEMG data were averaged across the targeted muscle groups and the target levels

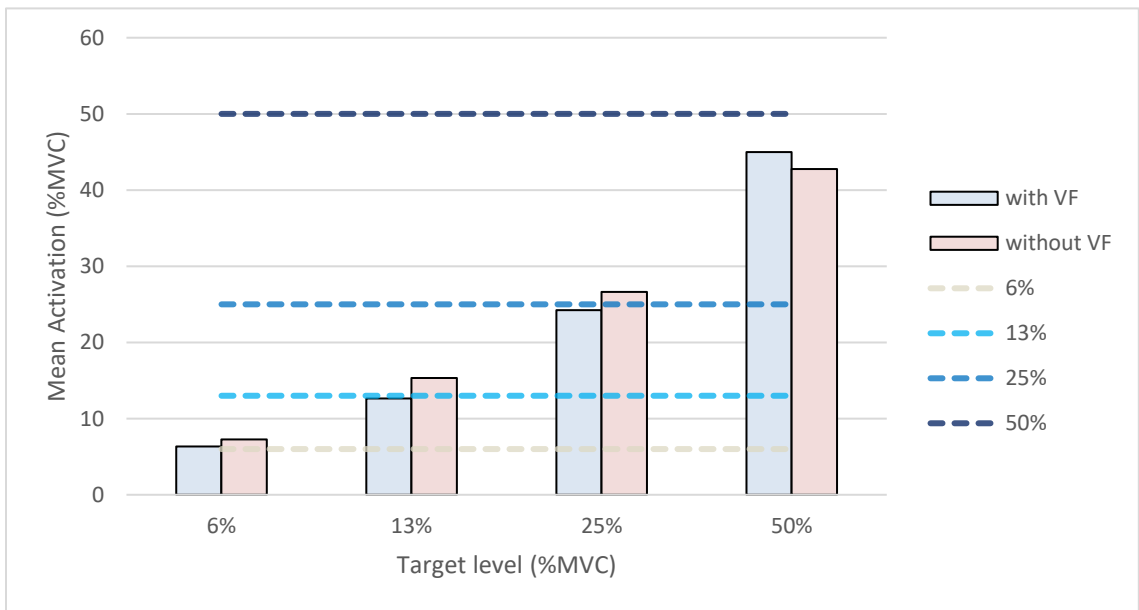


Figure 9 - Mean activation of muscle contraction for the target levels, the subject sEMG data were averaged across the muscle groups. Target levels were represented as dashed lines

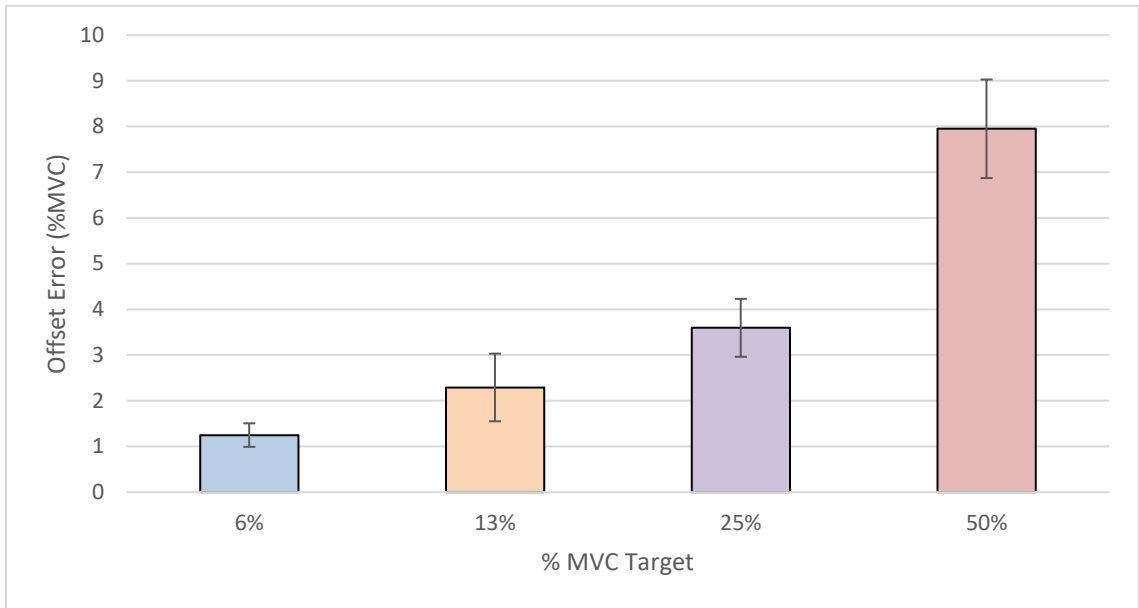


Figure 10 - Overall effect of %MVC (Target Intensity) on offset error; the subject sEMG data were averaged across the muscle groups and the presence or the absence of VF

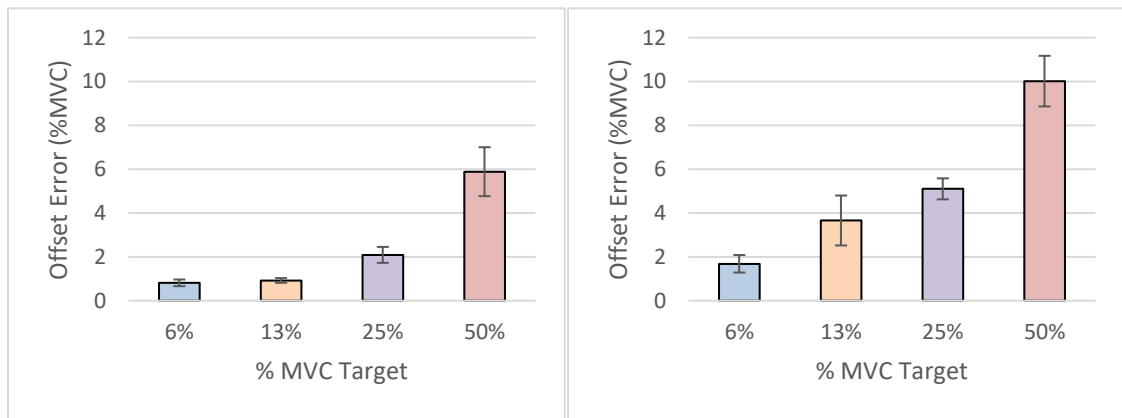


Figure 11 - Effect of %MVC (Target Intensity) on offset error depending on VF; left) with VF, right) without VF

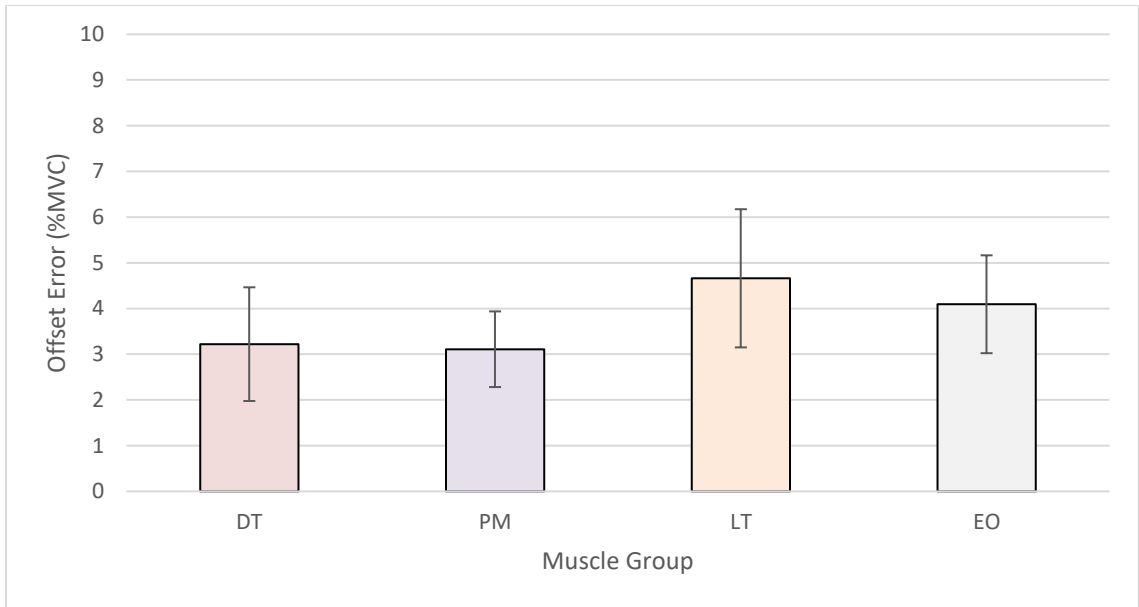


Figure 12 - Overall effect of Muscle group on offset error; the subject sEMG data were averaged across the target levels and the presence or the absence of VF

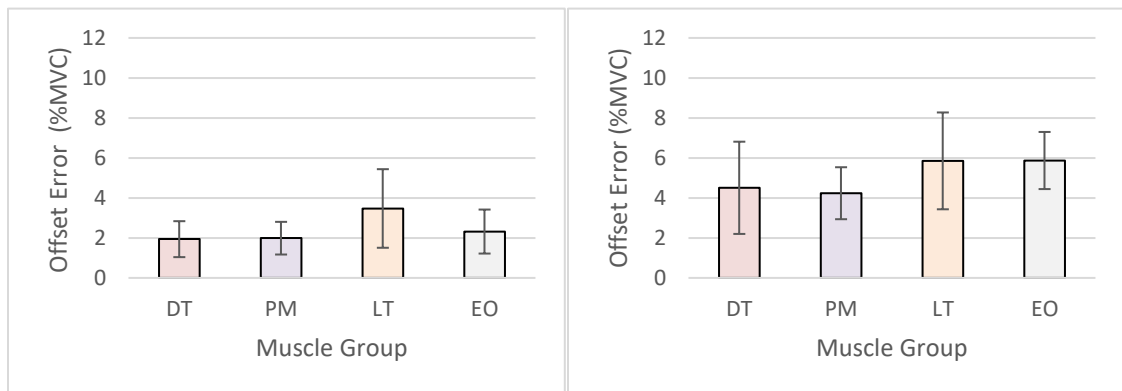


Figure 13 - Effect of Muscle group on offset error depending on VF; left) with VF, right) without VF

4.2 Variance Evaluation for Individual Muscle Contraction Stability

It is assumed that the variance at each target level would increase regardless of different muscle groups and target levels when the visual feedback was not allowed. Figure 14 showed a similar effect of visual feedback; the overall variance was increased without visual feedback as seen in the offset error analysis. Since high levels of variability in sEMG signals were normally observed with relatively weak muscle groups and with more intense muscle contractions, the variances were expected to increase in some muscle groups and in high target levels. To normalize the variances of sEMG data from different muscle groups and different target levels, the coefficient of variation was determined to represent the relative variability of each muscle contraction. As shown in Figure 15-16, relatively high variances occurred with higher intensities of target in both the presence or the absence of visual feedback. However, the coefficient of variation showed the similar trend across the target levels (Figure 17-18). The prominent effect of muscle groups on the variance was observed in PM and DT with the greatest and the least variance respectively; the similar variance trends were acquired with and without visual feedback. This means the variance and the relative variance were more affected by physiologically induced variations in each muscle group (Figure 19-22).

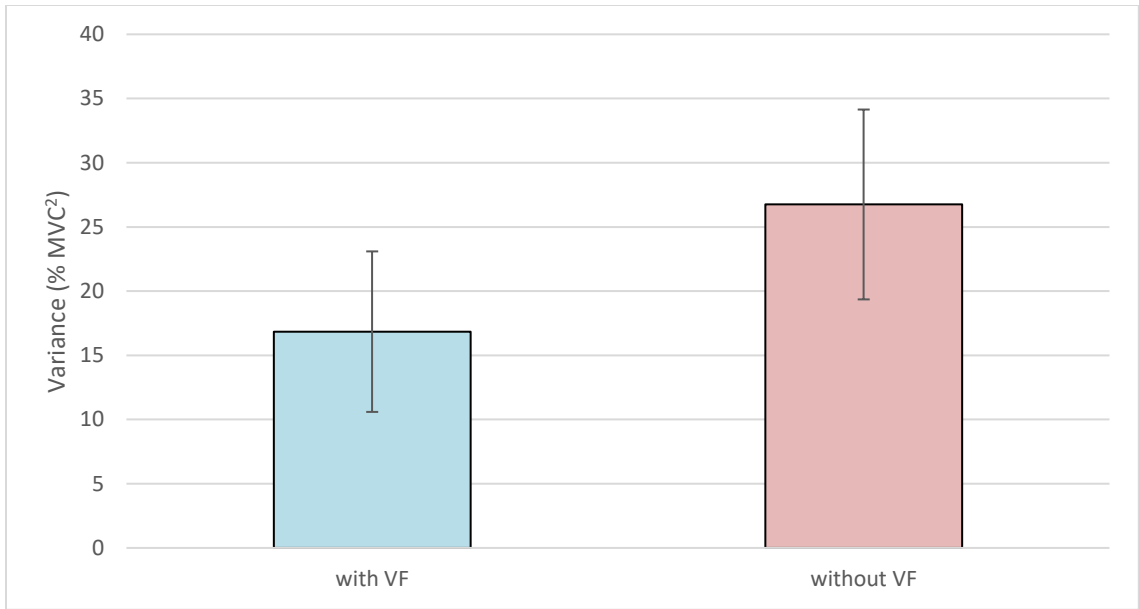


Figure 14 - Effect of Visual Feedback (VF) on variance; The subject sEMG data were averaged across the targeted muscle groups and the target levels

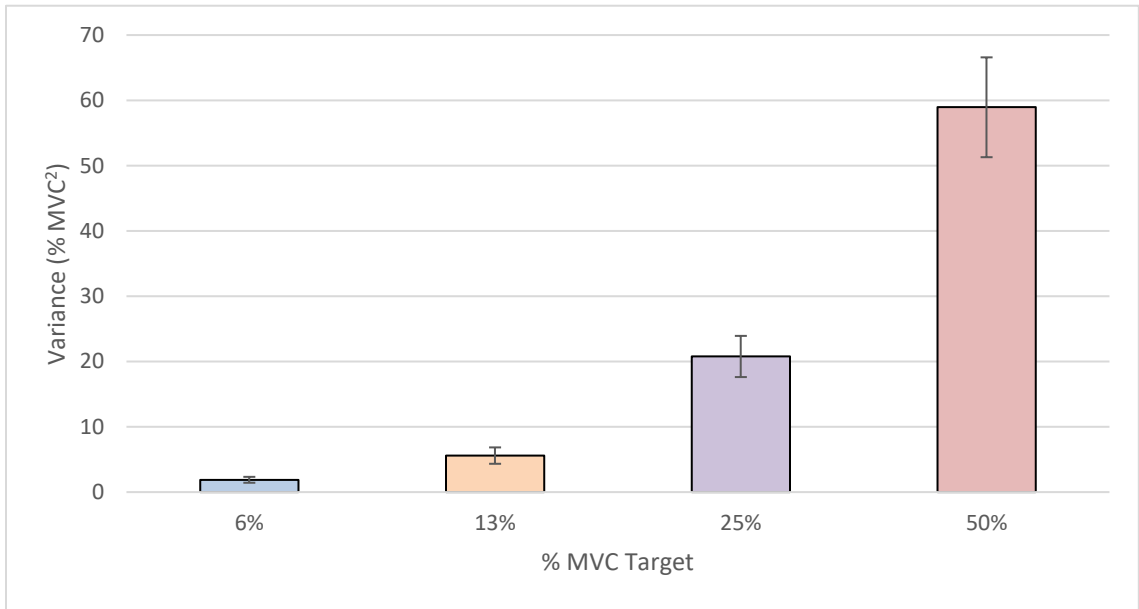


Figure 15 - Overall effect of %MVC (Target Intensity) on variance; the subject sEMG data were averaged across the muscle groups and the presence or the absence of VF

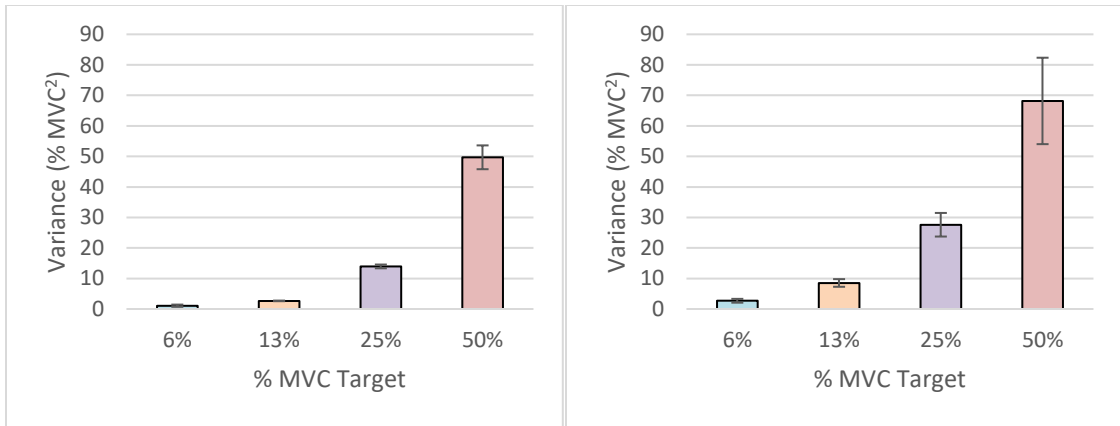


Figure 16 - Effect of % MVC (Target Intensity) on variance depending on VF; left) with VF, right) without VF

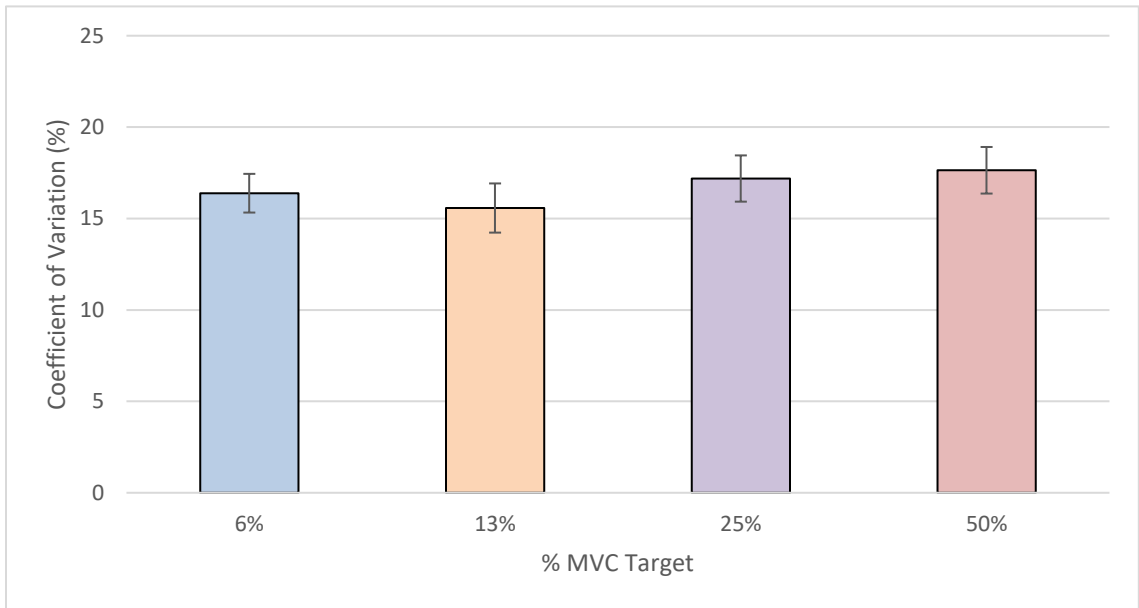


Figure 17 - Overall effect of %MVC (Target Intensity) on coefficient of variation; the subject sEMG data were averaged across the muscle groups and the presence or the absence of VF

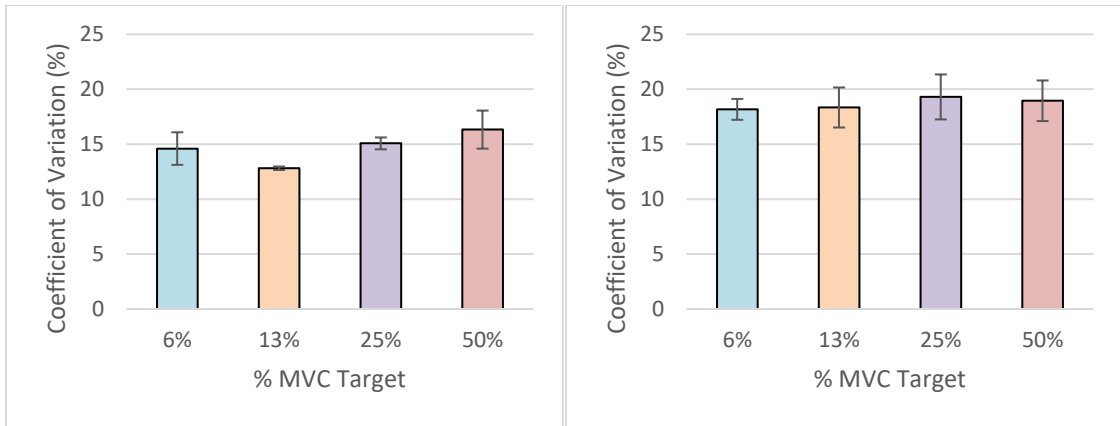


Figure 18 - Effect of %MVC (Target Intensity) on coefficient of variation depending on VF; left) with VF, right) without VF

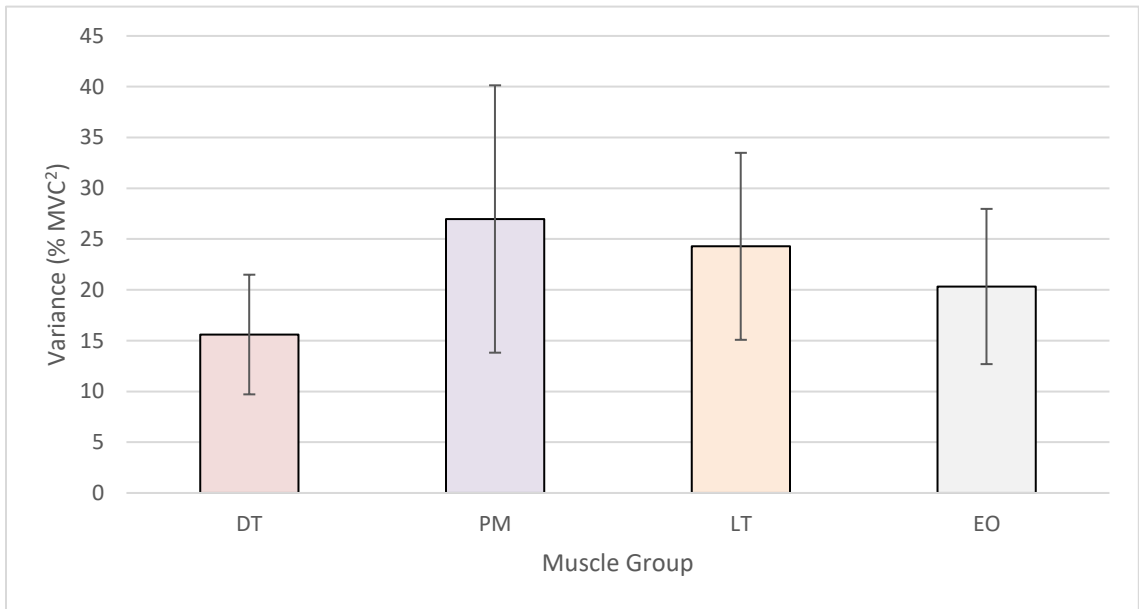


Figure 19 - Overall effect of Muscle group on variance; the subject sEMG data were averaged across the target levels and the presence or the absence of VF

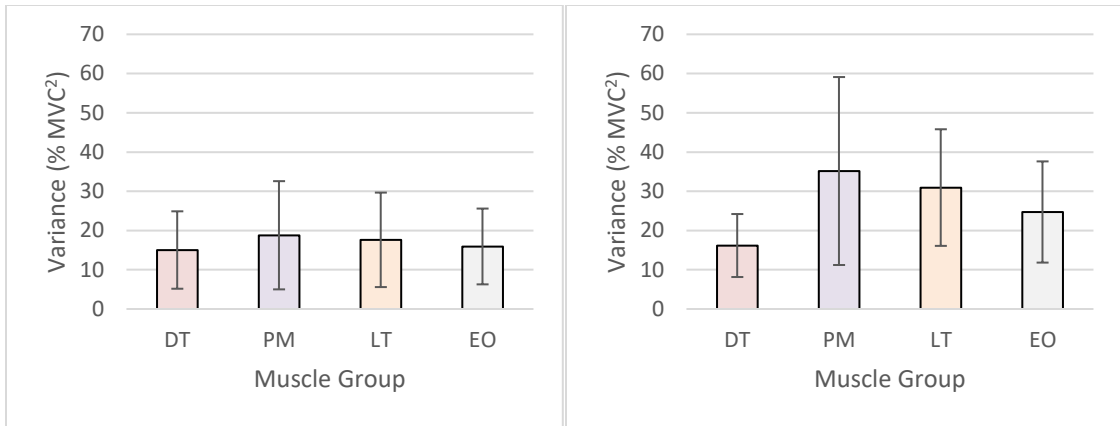


Figure 20 - Effect of Muscle group on variance depending on VF; left) with VF, right) without VF

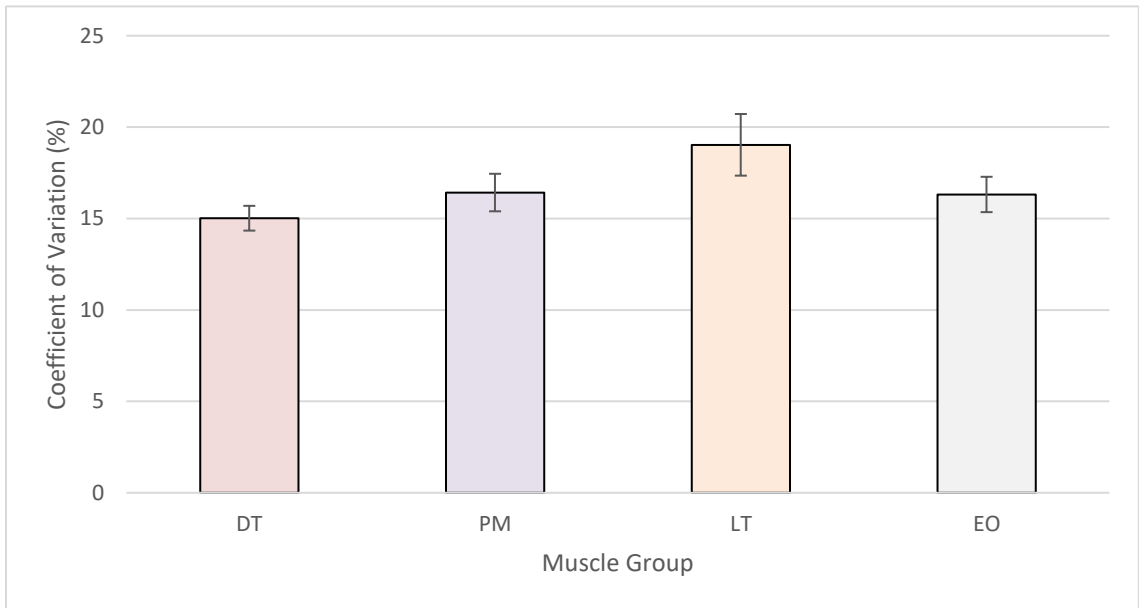


Figure 21 - Overall effect of Muscle group on coefficient of variation; the subject sEMG data were averaged across the target levels and the presence or the absence of VF

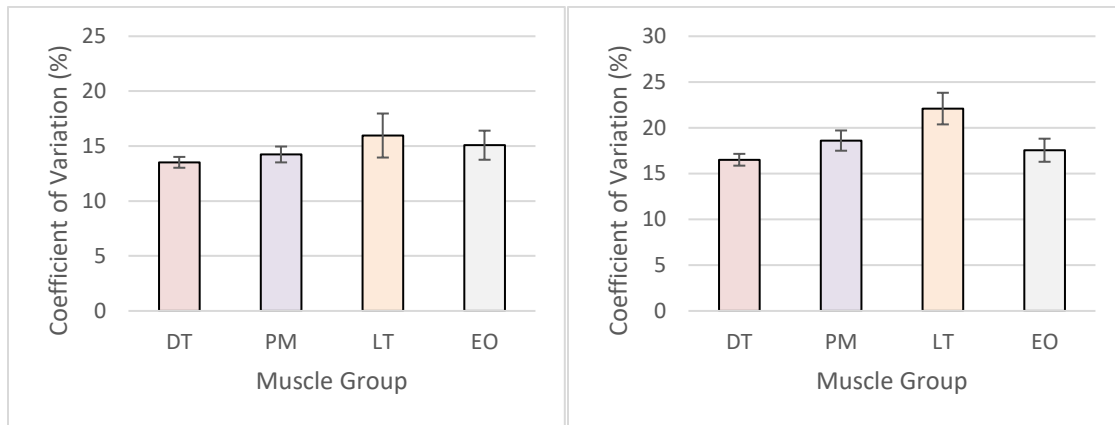


Figure 22 - Effect of Muscle group on coefficient of variation depending on VF; left) with VF, right) without VF

4.3 Contraction Bandwidth Evaluation for Individual Muscle Contraction

The contraction bandwidth of muscle contraction was evaluated by the time required for the targeted muscle to be contracted from 0% to 90% target and relaxed from 90% to 0% target. In contrast to the previous analysis on the offset error and the variance of the active state of muscle contraction, the transition phase of muscle activation was considered to determine the time required to fully activate or to relax the targeted muscle group. Although the auditory cues were given along with the visual feedback to indicate the initiation and the termination of the target muscle contraction, the interaction between the auditory cues and the visual feedback on muscle contraction time remained unknown. However, regardless of the visual feedback, the subject required more muscle activation time to reach higher target levels and to fully activate relatively weak muscle groups. Figure 23 showed that there was no substantial difference in the rise time, but the fall time was delayed by 100 ms when the visual feedback was not provided. The overall contraction time across the target levels was not affected by the visual feedback, and both rise and fall time gradually increased as the target level increased (Figure 24-25). The result across

different muscle groups also demonstrated that the effect of visual feedback on the contraction time was negligible. However, it was noted that the subject required more activation and relaxation time for DT compared to the other muscle groups and relatively less time for PM and EO. This implies that relatively fast muscle response can be achieved with the sEMG signals from PM and EO, and those muscles are more appropriate to apply to fast switching on/off control. Although DT showed relatively slow response, it is more suitable for precise and accurate control due to its low offset errors and variances at all different target levels (Figure 26-27).

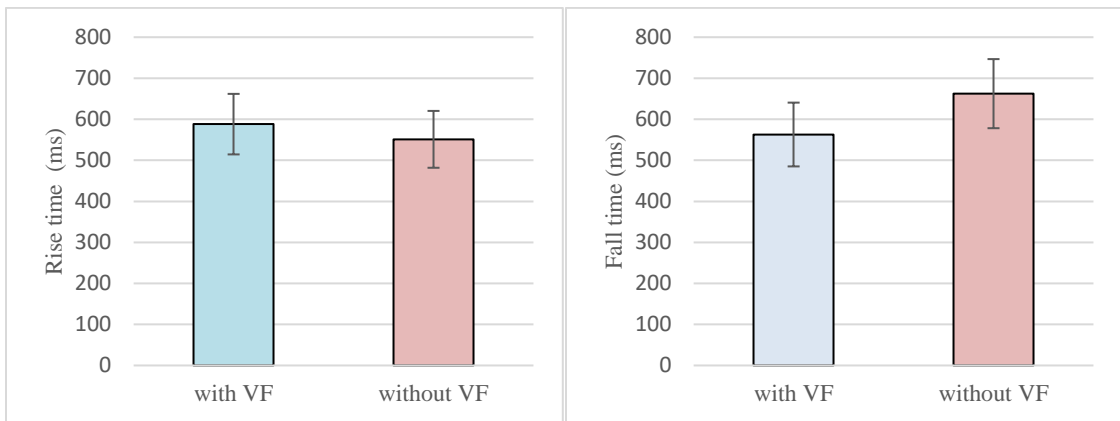


Figure 23 - Effect of Visual Feedback (VF) on rise time and fall time; The subject sEMG data were averaged across the targeted muscle groups and the target levels. Left) rise time, Right) fall time

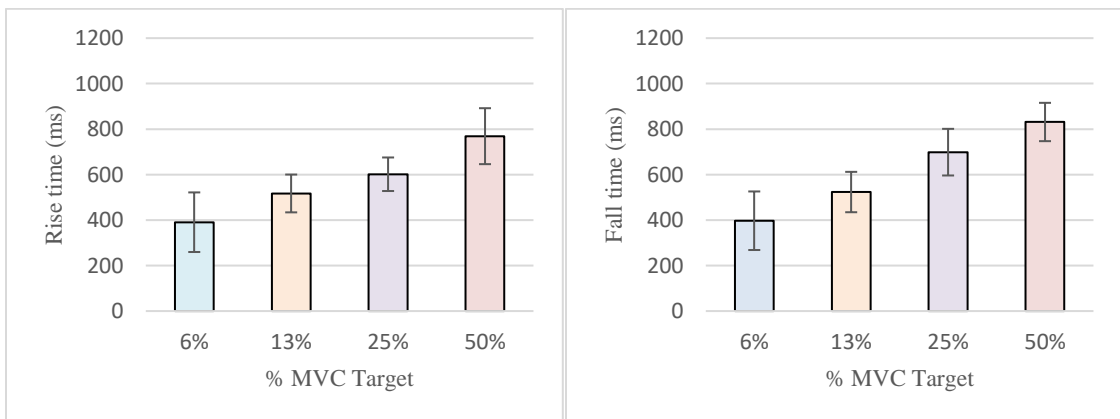


Figure 24 - Overall effect of % MVC (Target Intensity) on rise time and fall time; the subject sEMG data were averaged across the muscle groups and the presence or the absence of VF. Left) Rise time, Right) Fall time

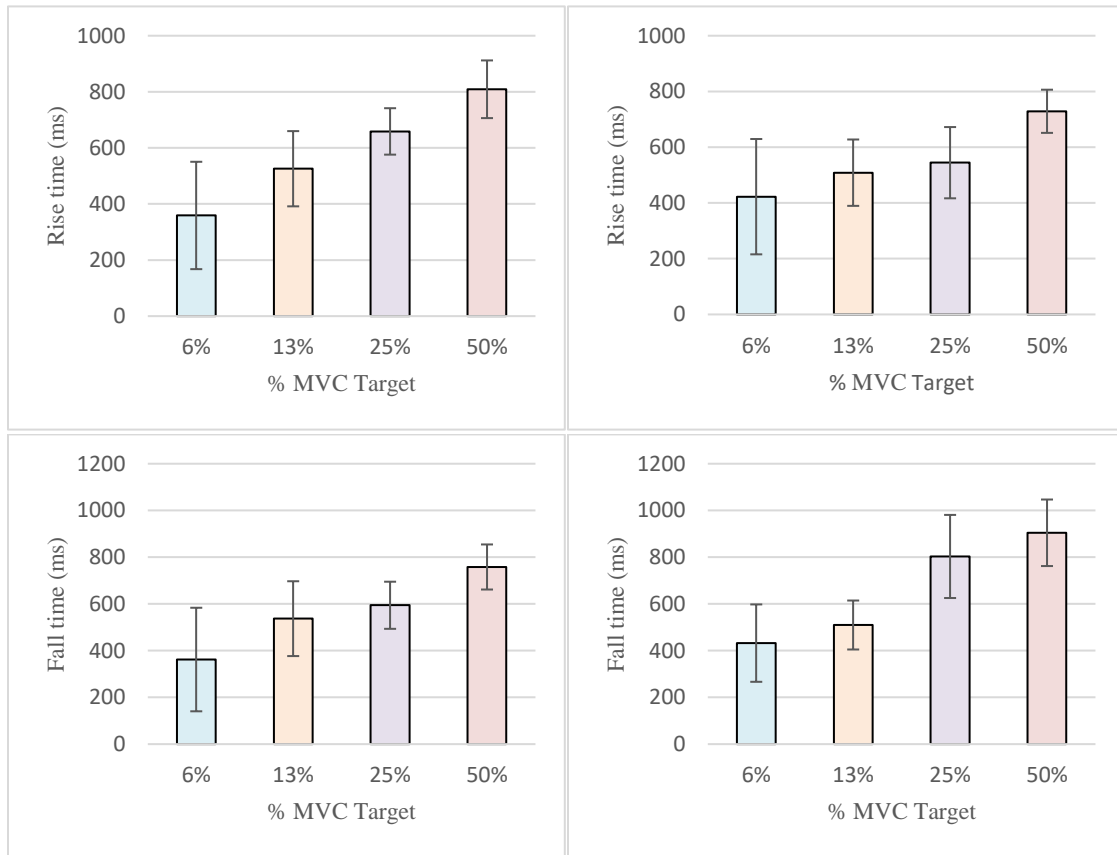


Figure 25 - Effect of % MVC (Target Intensity) on rise time and fall time depending on VF; Top left) Rise time with VF, Top right) Rise time without VF, Bottom left) Fall time with VF, Bottom right) Fall time without VF

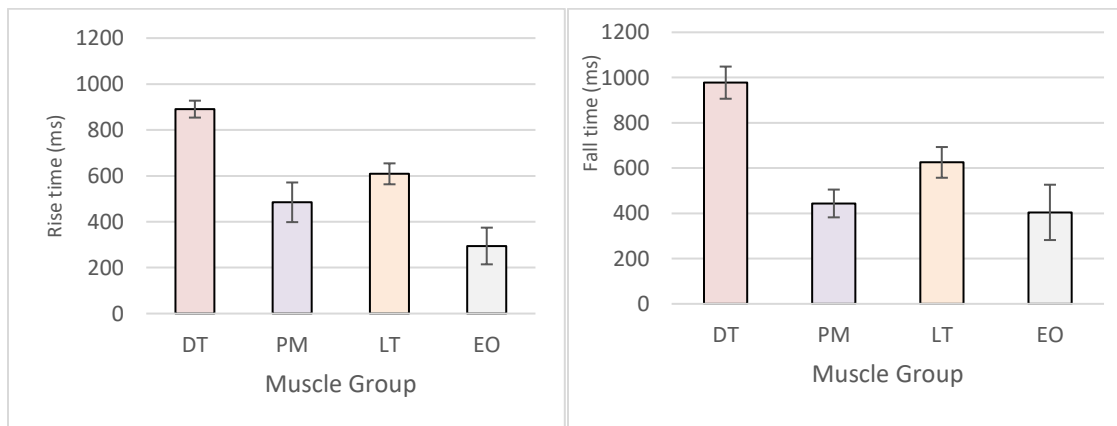


Figure 26 - Overall Effect of Muscle group on rise time and fall time; the subject sEMG data were averaged across the target levels and the presence or the absence of VF. Left) Rise time, Right) Fall time

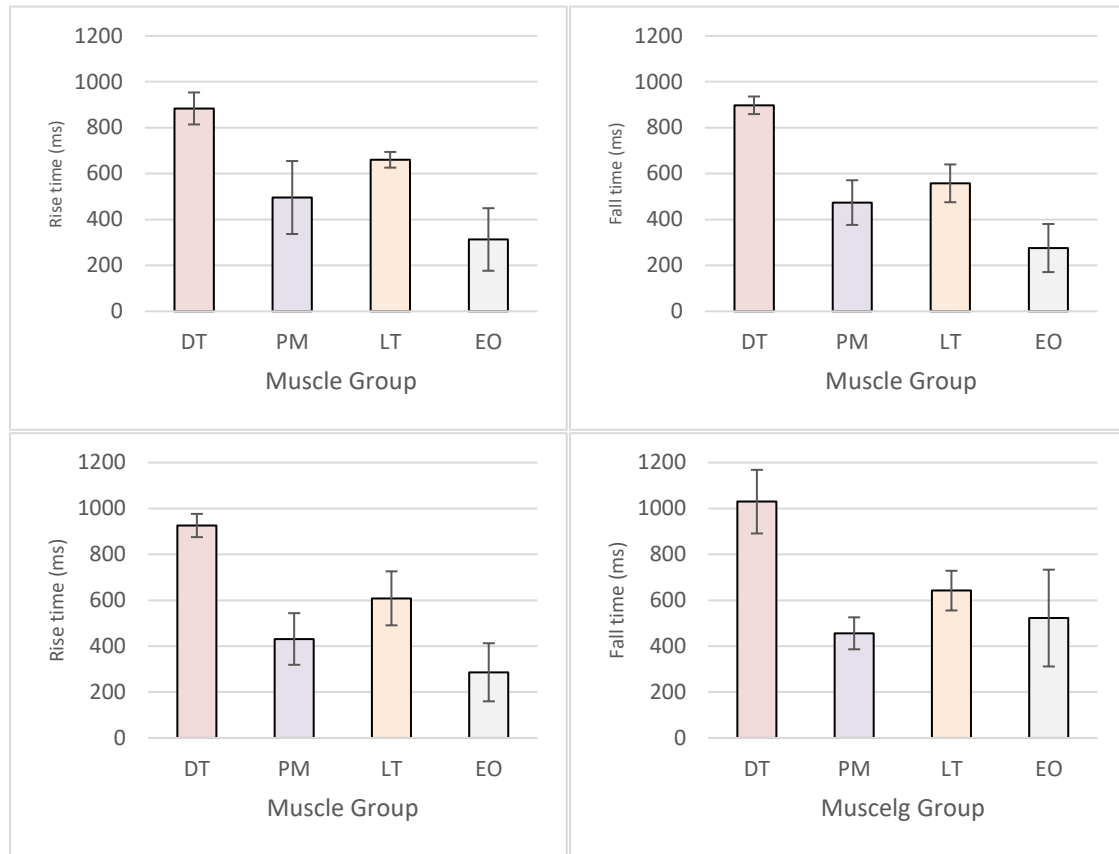


Figure 27 - Effect of Muscle group on rise time and fall time depending on VF; Top left) Rise time with VF, Top right) Rise time without VF, Bottom left) Fall time with VF, Bottom right) Fall time without VF

4.4 Evaluation of Simultaneous Muscle Contraction using LT and DT

The offset errors, the variances, and the contraction bandwidth of sEMG signals during simultaneous contraction were estimated to be higher than the individual muscle contraction, since it was more cognitively challenging to activate multiple muscles simultaneously. To investigate the anatomical correlation between the muscle groups, the sEMG signals were acquired from DT and LT which are the most and the least, respectively,

controllable muscle group in the upper body. Before evaluating the sEMG data, target combinations including LT 6% MVC + DT 6% MVC; LT 6% MVC + DT 25% MVC; LT 25% MVC + DT 6% MVC; and LT 25% MVC + DT 25% MVC were validated by the actual mean muscle activation as shown in Figure 28. Figure 29 showed the offset errors that occurred during the simultaneous muscle contraction and during the individual muscle contraction with LT and DT. Those values were also compared within the target level combinations. The offset errors in both LT and DT increased during simultaneous contraction. When the target levels for DT and LT were different, relatively high offset errors occurred in the muscle group with 25% MVC activation as seen in the individual contraction. And the offset errors in each muscle group drastically increased with the target level of 25% MVC for both LT and DT. Although the offset errors during the simultaneous contraction increased, it was noted that the offset error difference between LT and DT was maintained. For example, in the target combination of LT 25% + DT 25%, the offset error difference in the individual contraction was determined to be 2% and the same difference was observed in the simultaneous contraction. (Figure 30).

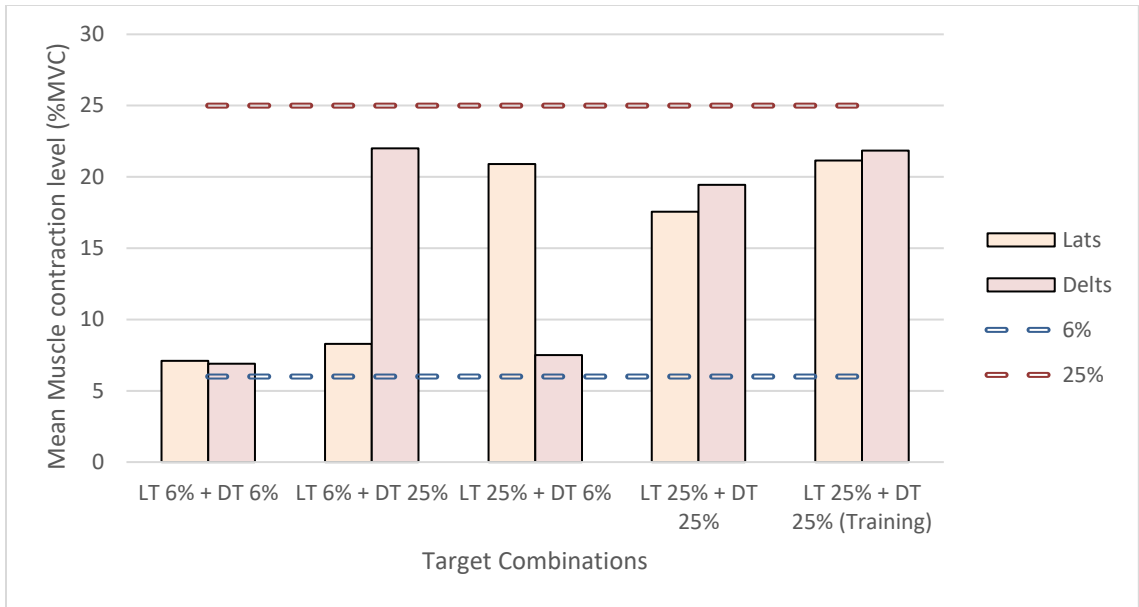


Figure 28 - Actual mean muscle activation for achieving each target combination; 6% MVC and 25% MVC were represented in blue and red dashed line respectively

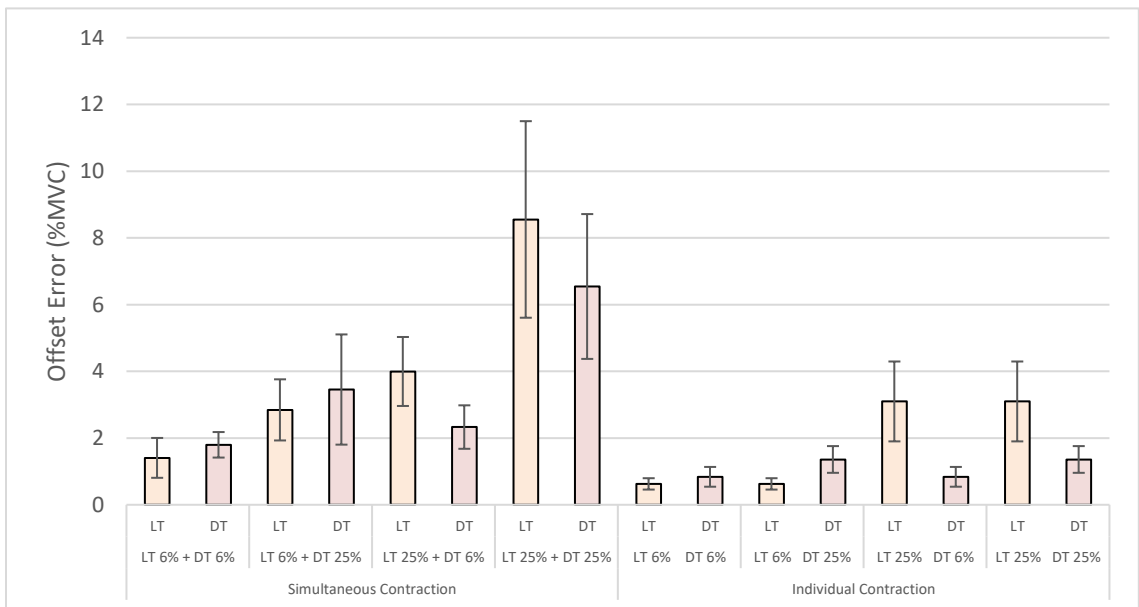


Figure 29 - The overall offset errors during simultaneous muscle contraction with LT and DT; The result was compared with the offset errors of individual muscle contractions

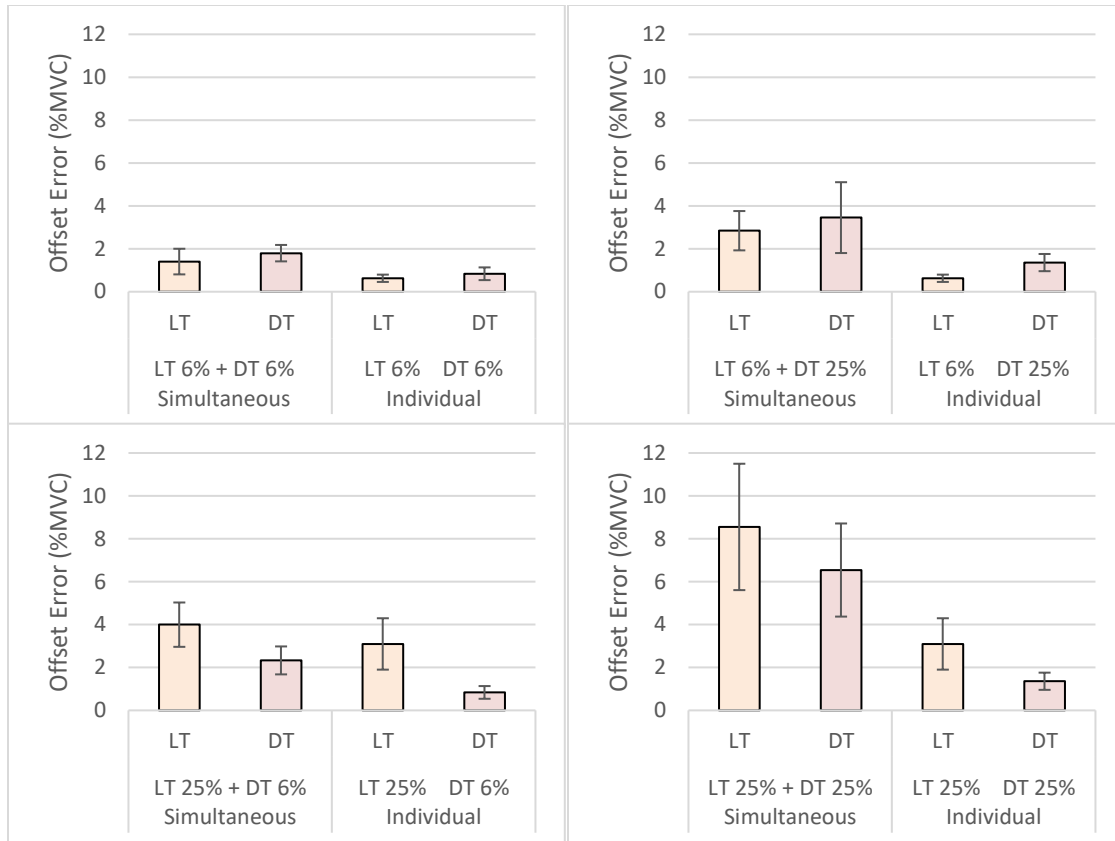


Figure 30 - The offset error comparison between the simultaneous and the individual muscle contraction for each target combination during simultaneous muscle contraction with LT and DT; Top left) LT 6% + DT 6%, Top right) LT 6% + DT 25%, Bottom left) LT 25% + DT

Figure 31-32 showed the variances during simultaneous contraction. Unlike the offset error, the variance displayed no substantial change overall. For the target combination of LT 6% + DT 6% in simultaneous contraction, the variances of LT and DT increased compared to the result found in individual contraction. However, when 25% MVC targets were required for both LT and DT, the variance in LT considerably increased while the variance in DT slightly decreased. For the target combinations with different target levels, the variance was reduced in the muscle group with 25% MVC target of the simultaneous contraction compared to the same muscle group of the individual contraction. Thus, when multiple

muscles were activated simultaneously, the minimum intensity of muscle activation was required to stabilize the muscle at the target level.

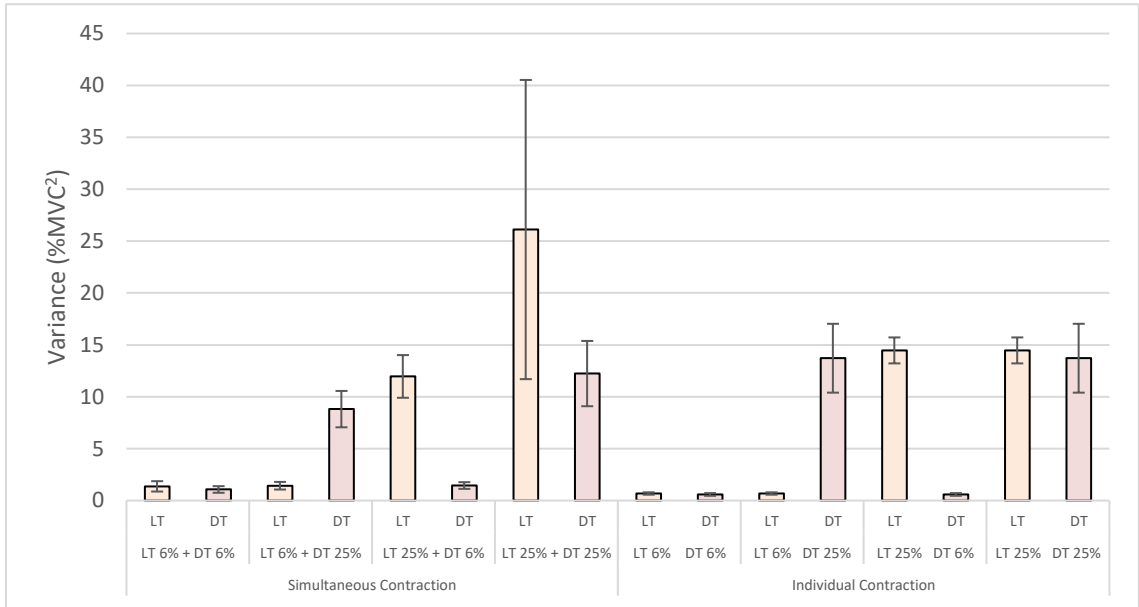


Figure 31 - The overall variances during simultaneous muscle contraction with LT and DT; The result was compared with the variances of individual muscle contractions

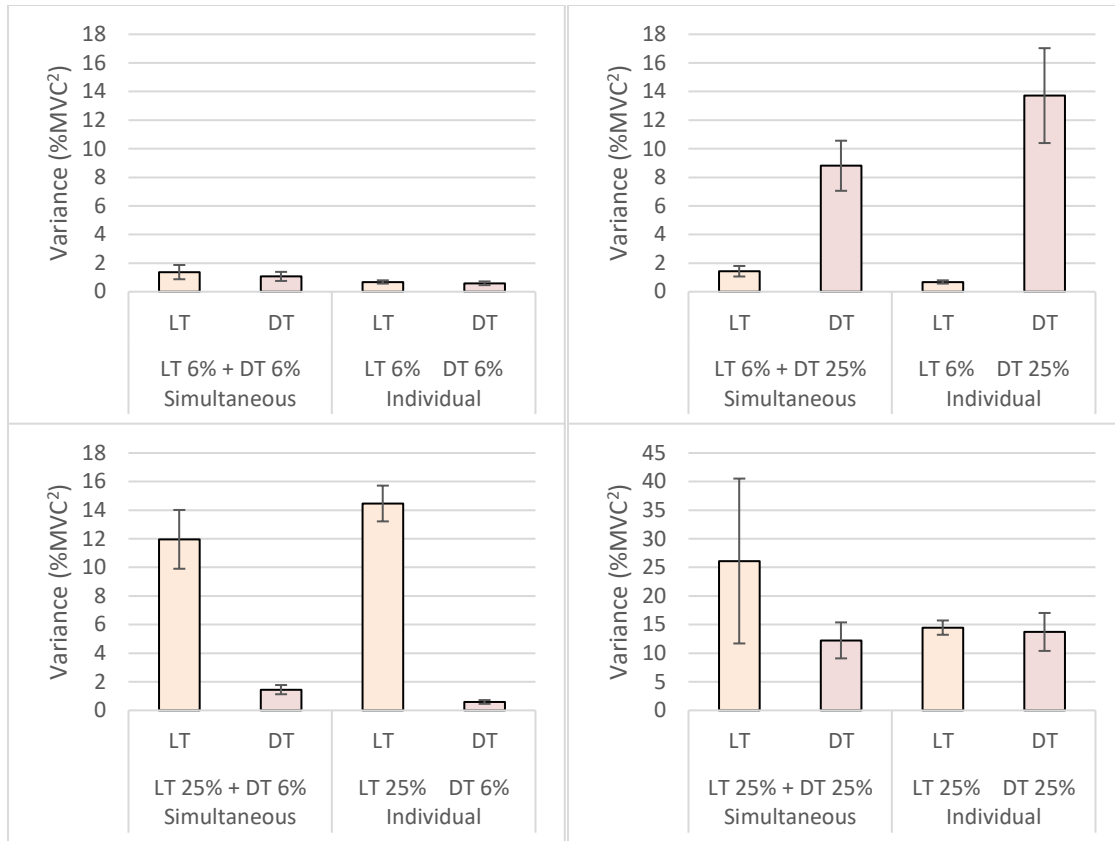


Figure 32 - The variances comparison between the simultaneous and the individual muscle contraction for each target combination during simultaneous muscle contraction with LT and DT; Top left) LT 6% + DT 6%, Top right) LT 6% + DT 25%, Bottom left) LT 25% + DT 6%,

The rise time and the fall time of LT and DT across different target combinations were also compared (Figure 33-35). Overall, the rise time of LT was shorter than the rise time of DT; similarly, the fall time of LT was shown to be shorter than the fall time of DT. During the simultaneous contraction, the intensity of targets in DT did not affect the rise time of LT for LT activation above 6% MVC, and it also did not affect the fall time of DT when the target in LT was fixed. Comparing the rise times of DT in both individual and simultaneous contraction, the most substantial delay was observed in LT 6%+DT 6%. But this delay was decreased when DT was activated to 25% MVC. Based on the results of rise

time and fall time during the simultaneous contraction, it was demonstrated that the minimum response time was required to activate LT and relax DT regardless of the activation level of the other.

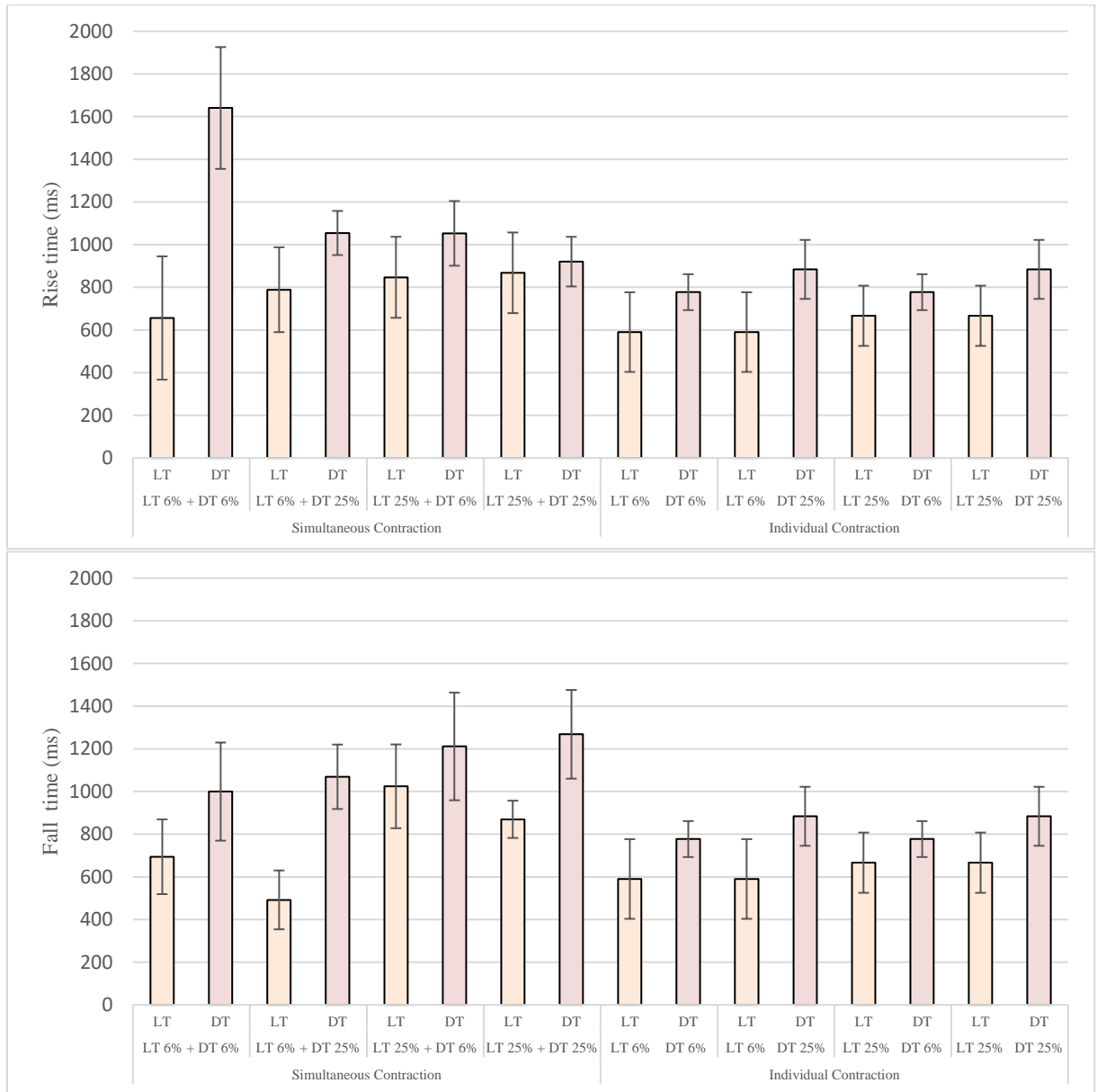


Figure 33 - Overall rise and fall time during simultaneous muscle contraction with LT and DT; The result was compared with the rise and fall time required for individual muscle contractions. Top) Rise time, Bottom) Fall time

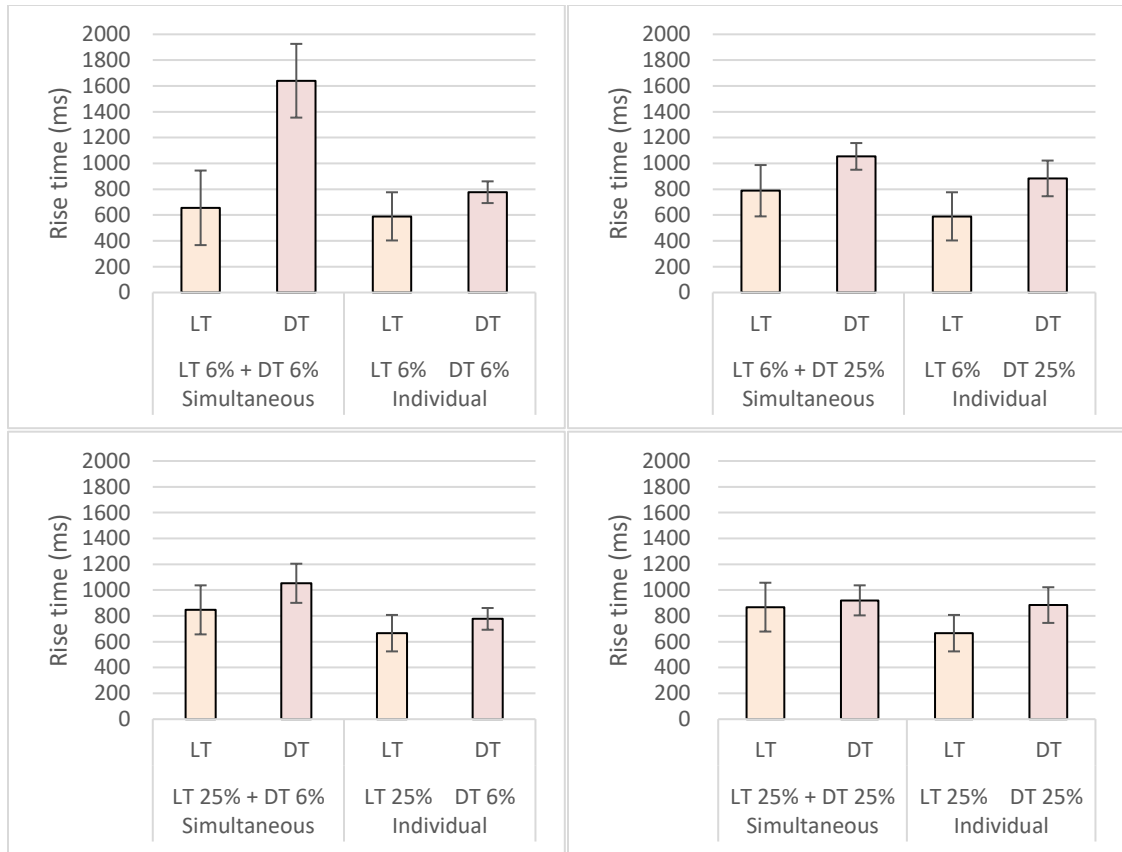


Figure 34 - The rise time comparison between the simultaneous and the individual muscle contraction for each target combination during simultaneous muscle contraction with LT and DT; Top left) LT 6% + DT 6%, Top right) LT 6% + DT 25%, Bottom left) LT 25% + DT 6%,

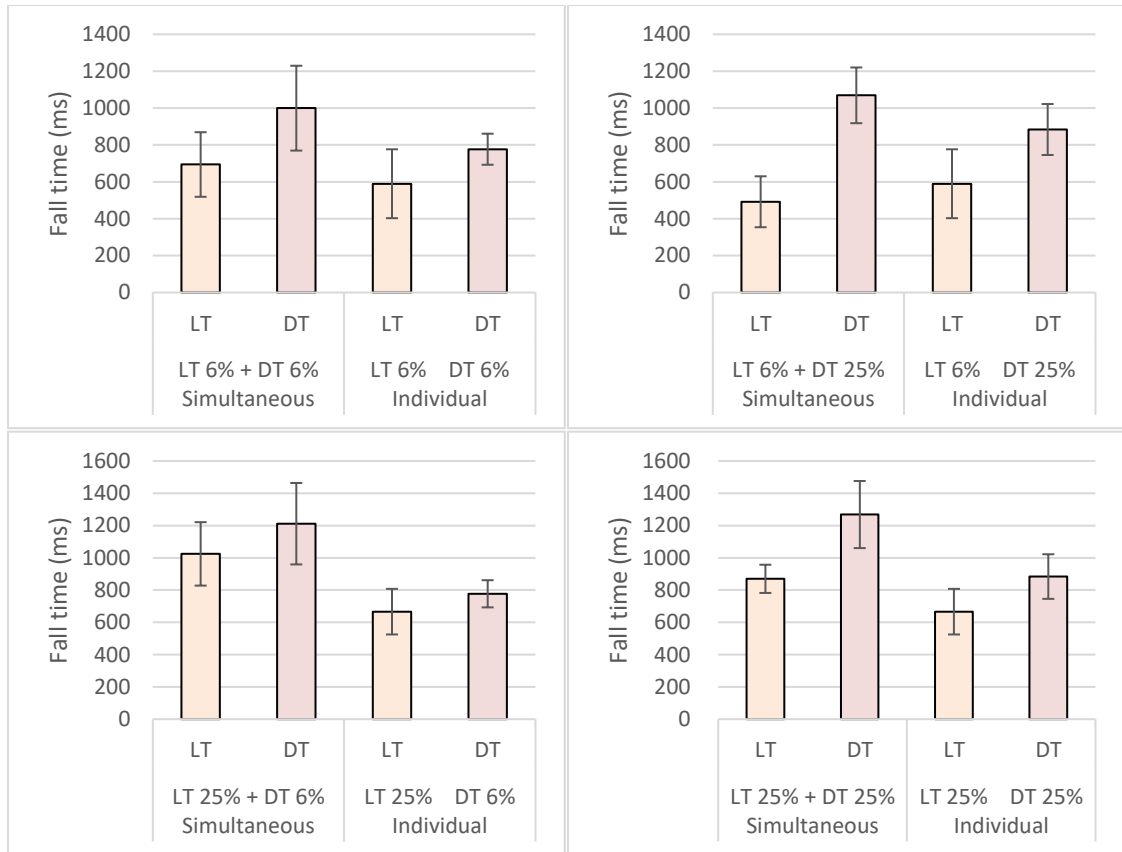


Figure 35 - The fall time comparison between the simultaneous and the individual muscle contraction for each target combination during simultaneous muscle contraction with LT and DT; Top left) LT 6% + DT 6%, Top right) LT 6% + DT 25%, Bottom left) LT 25% + DT 6%,

4.5 Post-training effect on the performance of simultaneous contraction

According to the subject's response to NASA Task Load Index, LT 25% + DT 25% was determined to be the worst-case combination. To investigate the effect of training on the performance of simultaneous contraction, the target combination of LT 25% + DT 25% was evaluated again after the training period for 10 minutes. The offset errors and the variances in LT were considerably reduced after training whereas those in DT did not. However, the subjects required more rise and fall time in both LT and DT compared to the simultaneous contraction before training (Figure 36-38).

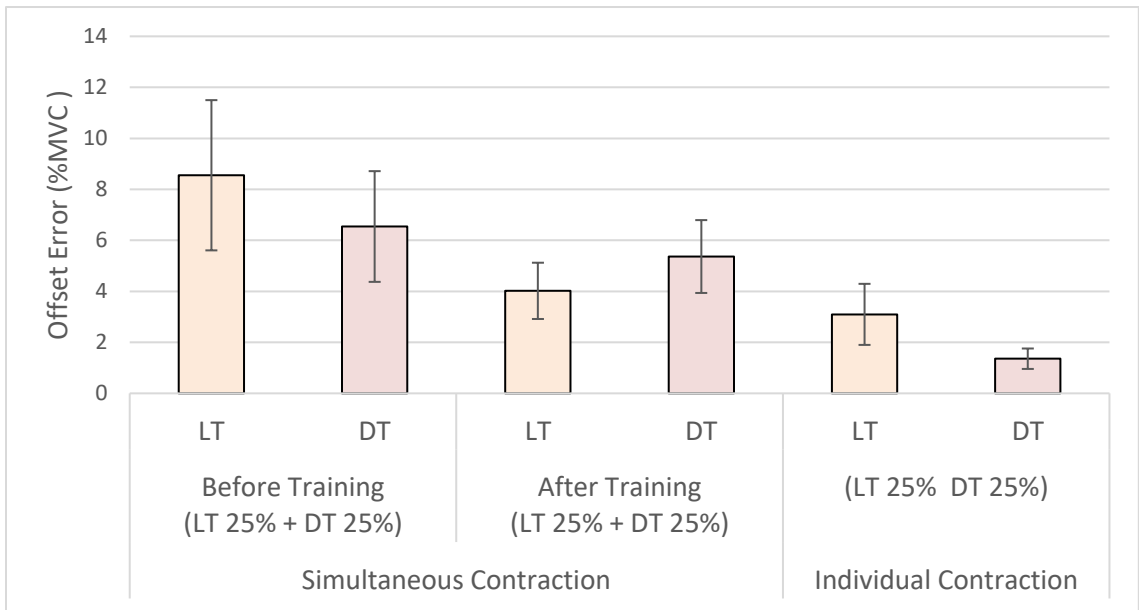


Figure 36 - Comparison on offset errors in LT and DT before and after training

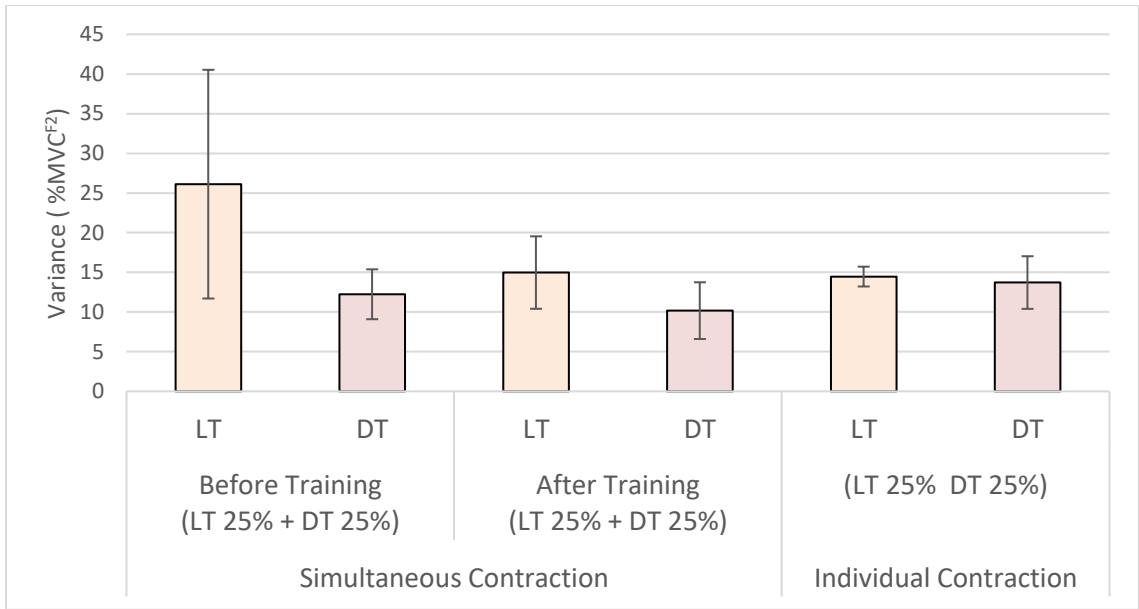


Figure 37 - Comparison on variances in LT and DT before and after training

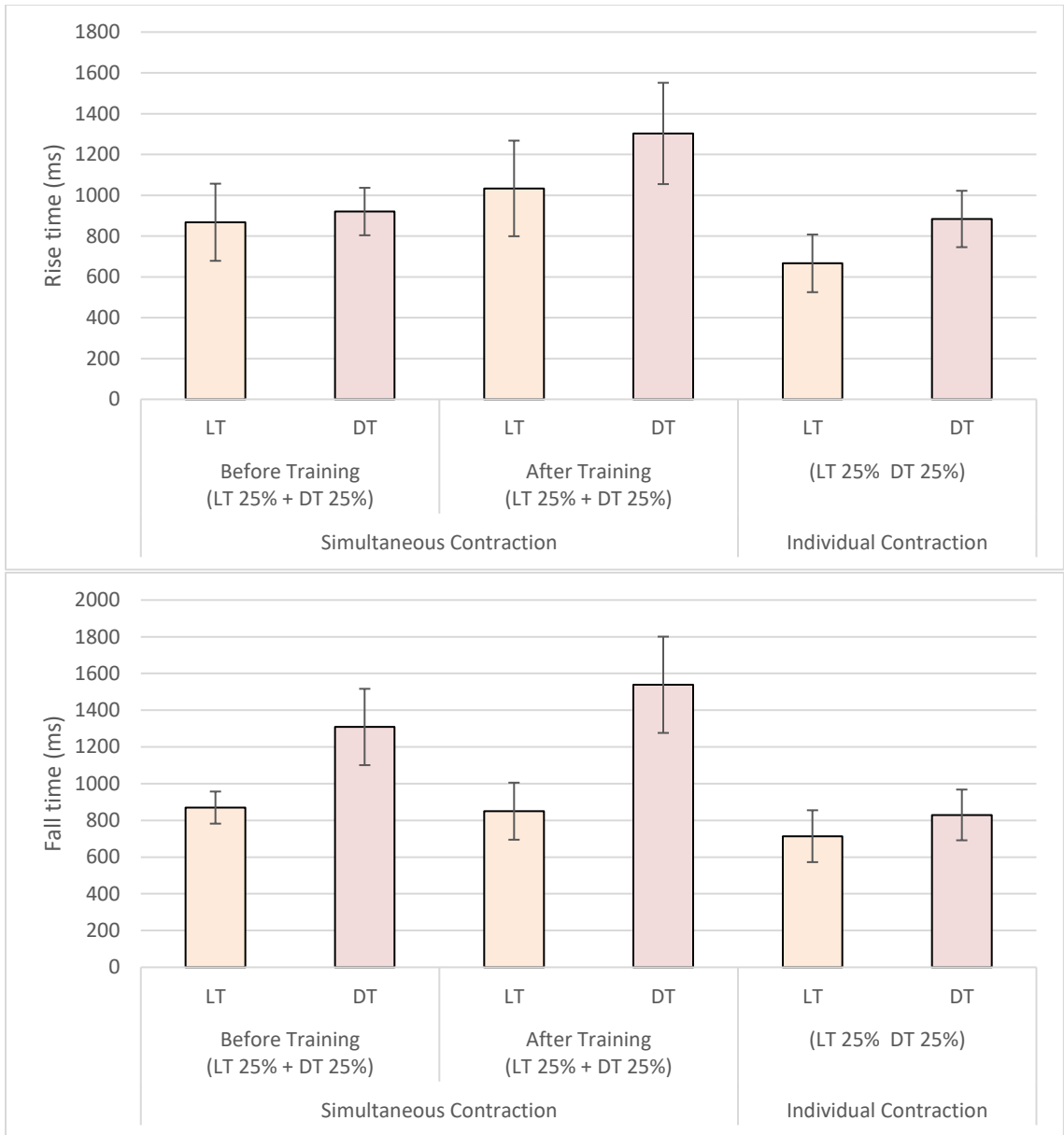


Figure 38 - Comparison on rise and fall time in LT and DT before and after training

CHAPTER 5. DISCUSSION AND CONCLUSION

5.1 Discussion

The experimental evaluation on the individual muscle contraction demonstrated that the human subject showed the enhanced muscle contraction performance with the visual feedback. While allowing the visual feedback, the designated targets were achieved within 10% offset deviation in all targeted muscle groups. This result demonstrated that the human subject's capability of generating 4 discrete sEMG output levels. Considering the offset deviation less than 10%, the subject had the possibility of generating more sEMG output levels. When comparing averages of offset errors from all targets in different muscle groups — DT, PM, LT, and EO — the relatively low offset errors occurred in DT and PM while the highest offset error occurred in LT regardless of the visual feedback. Therefore, it was recommended to use DT and PM to accurately control the desired sEMG output levels for the myoelectric prosthetic device control. Considering more muscular activities are triggered by intense muscle contraction, the variability of sEMG signals drastically increased when the target level was set to be 50% MVC. PM and LT were not recommended for applications that require precise operations, because, because they have shown higher variance levels than the other muscle groups. Although relatively low variances were observed in DT, it was still recommended using sEMG signals below 50% MVC to reduce the physiologically induced variation during muscle contractions. As the target levels increased, activation and relaxation times increased in the muscle groups. PM and EO had faster muscle responses, which indicated having faster switching on/off control, compared to LT and DT. Although DT showed slower response, it was more suitable for

the precise and accurate control due to its lower offset errors and variances at all target levels. Simultaneously activating multiple muscles required higher physical and mental demands compare to controlling muscles individually. Therefore, each muscle group had an increase in offset errors, variances, and time to activate and to relax. The higher offset errors were observed in the high activation muscle groups across all target combinations. However, the difference in the offset errors from individual contraction was maintained meaning that the human subject was able to activate LT and DT independently during simultaneous contractions. For the high activation muscle groups (for example, DT variance from LT 6% + DT 25%), the variances were lower in simultaneous contractions than in individual contractions. This indicated that the low activation muscle groups helped to lower the variances of the high activation muscle groups during the simultaneous contraction. Considering all target combinations in the rise and fall time, LT required less time than DT. The rise time of LT was independent of the intensity of DT while the rise time of DT was shortened in the higher target. The fall time of LT was diminished at DT target level 25% MVC, but the fall time of DT was consistent throughout different target levels. This result implied that the minimum of 25% MVC activation was necessary to achieve a quick manipulation in the prosthetic devices using LT and DT. The effects of the training were prominent in the offset error and the variance of LT than of DT. After the subject completed training, the increase in the rise time of LT and the fall time of DT helped to improve the offset error and the variance of LT.

5.2 Conclusion

This study investigated the sEMG signals of muscle groups in the upper body to evaluate the quality of voluntary muscle contraction in terms of the offset error, the variance level, and the contraction bandwidth. Based on the analysis of offset errors and variances from each muscle group, the presence of DT assisted more precise and stabilized manipulation. Fast responses of PM and EO suggested that these muscle groups were more suitable for a simple manipulation such as the on/off control than other muscle groups. This study focused on the sEMG output of 4 different combinations—LT and DT with 6% and 25% MVC respectively, and it demonstrated 4 discrete states of sEMG output can be achieved using LT and DT simultaneously. However, this study focused on the experimental evaluation of the voluntary muscle contraction performance of each individual muscle group. Therefore, the co-contraction occurred in non-targeted muscle groups during multiple DOF prosthetic control should be considered in the future study to investigate the synergistic effect of different muscle groups on multifunction myoelectric control. Furthermore, the possible combinations of various muscle groups and target levels needed to be tested to gather more sEMG outcomes with a bigger sample size for a reliable statistical analysis.

REFERENCES

- [1] Kwatny, E., Thomas, D. and Kwatny, H. (1970). An Application of Signal Processing Techniques to the Study of Myoelectric Signals. *IEEE Transactions on Biomedical Engineering*, BME-17(4), pp.303-313.
- [2] Young, A., Smith, L., Rouse, E. and Hargrove, L. (2014). A comparison of the real-time controllability of pattern recognition to conventional myoelectric control for discrete and simultaneous movements. *Journal of NeuroEngineering and Rehabilitation*, 11(1), p.5.
- [3] Scheme, E., Englehart, K. and Hudgins, B. (2011). Selective Classification for Improved Robustness of Myoelectric Control Under Nonideal Conditions. *IEEE Transactions on Biomedical Engineering*, 58(6), pp.1698-1705.
- [4] Englehart, K. and Hudgins, B. (2003). A robust, real-time control scheme for multifunction myoelectric control. *IEEE Transactions on Biomedical Engineering*, 50(7), pp.848-854.
- [5] L. Hargrove, E. Scheme, K. Englehart and B. Hudgins, "Multiple Binary Classifications via Linear Discriminant Analysis for Improved Controllability of a Powered Prosthesis", *IEEE Transactions on Neural Systems and Rehabilitation Engineering*, vol. 18, no. 1, pp. 49-57, 2010.
- [6] E. Scheme and K. Englehart, "Electromyogram pattern recognition for control of powered upper-limb prostheses: State of the art and challenges for clinical use", *The Journal of Rehabilitation Research and Development*, vol. 48, no. 6, p. 643, 2011.
- [7] M. Yokoyama and M. Yanagisawa, "Logistic Regression Analysis of Multiple Interosseous Hand-Muscle Activities using Surface Electromyography during Finger-Oriented Tasks," Dec. 2018.
- [8] V. H. Cene and A. Balbinot, "Upper-limb movement classification through logistic regression sEMG signal processing," 2015 Latin America Congress on Computational Intelligence (LA-CCI), 2015.
- [9] R. Merletti, L. Lo Conte, E. Avignone and P. Guglielminotti, "Modeling of surface myoelectric signals. I. Model implementation", *IEEE Transactions on Biomedical Engineering*, vol. 46, no. 7, pp. 810-820, 1999.
- [10] A. Adewuyi, L. Hargrove and T. Kuiken, "An Analysis of Intrinsic and Extrinsic Hand Muscle EMG for Improved Pattern Recognition Control", *IEEE Transactions on Neural Systems and Rehabilitation Engineering*, vol. 24, no. 4, pp. 485-494, 2016.

- [11] C. De Luca, "Physiology and Mathematics of Myoelectric Signals", *IEEE Transactions on Biomedical Engineering*, vol. -26, no. 6, pp. 313-325, 1979.
- [12] R. Merletti, *Electromyography: Physiology, Engineering and Non-Invasive Applications*. John Wiley & Sons, 2004.
- [13] O. Samuel, H. Zhou, X. Li, H. Wang, H. Zhang, A. Sangaiah and G. Li, "s", *Computers & Electrical Engineering*, vol. 67, pp. 646-655, 2018.
- [14] A. Al-Timemy, G. Bugmann, J. Escudero and N. Outram, "Classification of Finger Movements for the Dexterous Hand Prosthesis Control With Surface Electromyography", *IEEE Journal of Biomedical and Health Informatics*, vol. 17, no. 3, pp. 608-618, 2013.
- [15] I. Vujaklija, V. Shalchyan, E. Kamavuako, N. Jiang, H. Marateb and D. Farina, "Online mapping of EMG signals into kinematics by autoencoding", *Journal of NeuroEngineering and Rehabilitation*, vol. 15, no. 1, 2018.
- [16] E. Mastinu, J. Ahlberg, E. Lendaro, L. Hermansson, B. Hakansson and M. Ortiz-Catalan, "An Alternative Myoelectric Pattern Recognition Approach for the Control of Hand Prostheses: A Case Study of Use in Daily Life by a Dysmelia Subject", *IEEE Journal of Translational Engineering in Health and Medicine*, vol. 6, pp. 1-12, 2018.
- [17] G. Li, Y. Li, L. Yu and Y. Geng, "Conditioning and Sampling Issues of EMG Signals in Motion Recognition of Multifunctional Myoelectric Prostheses", *Annals of Biomedical Engineering*, vol. 39, no. 6, pp. 1779-1787, 2011.
- [18] A. Roche, H. Rehbaum, D. Farina and O. Aszmann, "Prosthetic Myoelectric Control Strategies: A Clinical Perspective", *Current Surgery Reports*, vol. 2, no. 3, 2014.
- [19] N. Fallahian, H. Saeedi, H. Mokhtarinia and F. Tabatabai Ghomshe, "Sensory feedback add-on for upper-limb prostheses", *Prosthetics and Orthotics International*, vol. 41, no. 3, pp. 314-317, 2016. Available: 10.1177/0309364616677653.
- [20] J. Schofield, K. Evans, J. Carey and J. Hebert, "Applications of sensory feedback in motorized upper extremity prosthesis: a review", *Expert Review of Medical Devices*, vol. 11, no. 5, pp. 499-511, 2014. Available: 10.1586/17434440.2014.929496.
- [21] J. Lee, M. H. Choi, J. H. Jung, and F. L. Hammond, "Multimodal sensory feedback for virtual proprioception in powered upper-limb prostheses," *2017 26th IEEE International Symposium on Robot and Human Interactive Communication (RO-MAN)*, 2017.

- [22] A. M. Hart, L. O. Tiziani, J. H. Jung, and F. L. Hammond, "Deformable reflective diaphragm sensors for control of soft pneumatically actuated devices," *2018 IEEE International Conference on Soft Robotics (RoboSoft)*, 2018.
- [23] J. Ives and J. Wigglesworth, "Sampling rate effects on surface EMG timing and amplitude measures", *Clinical Biomechanics*, vol. 18, no. 6, pp. 543-552, 2003.
- [24] P. Komi and P. Tesch, "EMG frequency spectrum, muscle structure, and fatigue during dynamic contractions in man", *European Journal of Applied Physiology and Occupational Physiology*, vol. 42, no. 1, pp. 41-50, 1979.
- [25] Reaz, M., Hussain, M. and Mohd-Yasin, F. (2006). Techniques of EMG signal analysis: detection, processing, classification and applications (Correction). *Biological Procedures Online*, 8(1), pp.163-163.
- [26] E. Rocha, D. Cantergi, A. Santos, D. Soares, C. Candotti and J. Loss, "Smoothing EMG signals: implications on delay calculation", *Revista Portuguesa de Ciências do Desporto*, vol. 12, no. 1, pp. 60-72, 2012.
- [27] A. Jette, "The Promise of Assistive Technology to Enhance Work Participation", *Physical Therapy*, vol. 97, no. 7, pp. 691-692, 2017.
- [28] F. Cordella, A. Ciancio, R. Sacchetti, A. Davalli, A. Cutti, E. Guglielmelli and L. Zollo, "Literature Review on Needs of Upper Limb Prosthesis Users", *Frontiers in Neuroscience*, vol. 10, 2016.
- [29] X. Zhang, X. Ren, X. Gao, X. Chen and P. Zhou, "Complexity Analysis of Surface EMG for Overcoming ECG Interference toward Proportional Myoelectric Control", *Entropy*, vol. 18, no. 4, p. 106, 2016.
- [30] P. Zhou and X. Zhang, "A novel technique for muscle onset detection using surface EMG signals without removal of ECG artifacts", *Physiological Measurement*, vol. 35, no. 1, pp. 45-54, 2013.
- [31] S. Solnik, P. Rider, K. Steinweg, P. Devita, and T. Hortobágyi, "Teager–Kaiser energy operator signal conditioning improves EMG onset detection," *European Journal of Applied Physiology*, vol. 110, no. 3, pp. 489–498, 2010.
- [32] "Compex Muscle Stimulators for Sport, Training & Recovery", *Compex*, 2018. [Online]. Available: <https://www.compex.com/electrode-placements>. [Accessed: 10-Dec-2018].
- [33] "Best Electrode Placement For Arm and Hand Stroke Rehabilitation," *NeuroRehab Directory*, 07-May-2017. [Online]. Available: <https://www.neurorehabdirectory.com/electrode-placement/>. [Accessed: 10-Dec-2018].